A Center for Advanced Materials and Nanotechnology in AMRI at the University of New Orleans

Louisiana Board of Regents Contract LEQSF(2007-12)-ENH-PKSFI-PRS-04

Annual Progress Report - 2009

June 30, 2009

SUMMARY

The purpose of this report is to provide an annual progress report for the LA Board of Regents funded project entitled: "A Center for Advanced Materials and Nanotechnology in AMRI at the University of New Orleans" through LA Board of Regents Contract LEQSF(2007-12)-ENH-PKSFI-PRS-04 during the second year of the project from July 1, 2008, through June 30, 2009. Included are progress reports from the three Focus Research Groups (FRGs) and the Broader Impacts group which comprise the organization of the overall project, plus a progress report on the Clean Room Project for which received ESIP funds for development of a Nanodevice Processing Laboratory to support ongoing research projects in nanotechnology at UNO.

The second year of this project was very productive and has been successfully completed. A research consortium organization for this project continues in place and includes as participants the University of New Orleans and the following five partner institutions: Louisiana State University, Tulane University, Louisiana Tech University, Children's Hospital, and Communities in Schools of New Orleans, Inc. The subcontracts from the University of New Orleans to the five collaborating partner institutions continue in place and the work at these institutions is progressing well. The overall effort of the project is organized into three FRGs based on technical areas and one Broader Impacts group, which provides community outreach support for the project. These groups are: FRG-1: Nanomaterials for Biological Sensing and Imaging; FRG-2: Nanoscale Mechanical Devices; FRG-3: Nanomaterials for Energy Conversion and Storage; and the Broader Impacts (Educational and Commercial Outreach) group. All research activities within each group are progressing well.

Report for LEQSF(2009-06)-ENH-PKSFI-PRS-04

Weilie Zhou

(PKSFI FRG 1, 2008-2009)

1. Personnel: List all key personnel and other staff who provided *significant* contributions to the project. Provide information about the types of contributions made by each listed participant and controls in place to ensure that these contributions are adequate to the project's requirements.

A. AMRI personnel involves with this project

- **Weilie Zhou**- co-Leader of FRG 1. He is mainly responsible for overall management for biosensor part and coordination of AMRI tasks with other partners
- **Zhongming Zeng**-Postdoctoral Research Associate; Zhongming is in charge of nanowire assemble, e-beam nanolithography, and detection of antigen fabricated from Children Hospital of LSUHSC.
- **Hui Ma**-Ph.D student: She is fabricating magnetic nanocarriers for drug delivery and meanwhile she is in charge of modifying the nanowire surface for bio-detection.
- **Charles J O'Connor**-Principal investigator, investigating the whole project and looking for the new grant for whole teams. He is also directing magnetic nanoparticle synthesis.
- **Daniela Caruntu**-Postdoctoral Research Associate; She is in charge of magnetic nanoparticle synthesis for biomedical application.
- **Zeev Rosenzweig**-Professor in Chemistry, His group is fabricating quantum dots for biomedical imaging.

B. CAMD personnel involved with this project

- **Jost Goettert** – main responsibility is overall project management for CAMD part and coordination of CAMD tasks with partner efforts;
- **Yoonyoung Jin** – Research Associate (RA); Jin is leading senior researcher at CAMD with expertise in lithography, thin films, system integration, and measurements; he was carrying out RIE process and was in charge of the rapid prototyping solutions for microfluidic;
- **Kyung-Nam Kang** – PhD student; he is supporting Jin with lithography and thin film deposition/etching related processing;
- **Proyag Datta** – Research Associate (RA) 5; he joined the team in the last 2 months providing expertise in molded microfluidic structures and fluidic system control and integration; he is currently molding hard plastic fluidic chips and works on chip integration with Si sensors.

C. LSUHSC Children Hospital involved with this project

- **Seth Pincus**-co-leader of this project. He is responsible for antigen engineering.
- **Chad Gustafson** (50%) **–** Bachelor's level Technician, working on the engineering
- **Grace Maresh** –Technician, working on quantum imaging.

D. Louisian Tech personnel involved with this project

- **Mark DeCoster**-Professor in biochemistry; he is in charge of biocompatible testing and alive cell detection
- **James McNamara**-Ph.D student; he is in charge of alive cell culture and testing
- **Ruturaj Masvekar**- M.S student; he is responsible for toxicity test for magnetic carriers and nanowires

2. **Activities and Findings:**

I. Metal Oxide Nanowire for biosensor application

A. Field effect transistor fabrication based on In_2O_3 nanowires

In the second year, we have improved the In_2O_3 nanowire field-effect transistors (FET) by bottom-up method. The In_2O_3 nanowire devices were fabricated into FETs by e-beam lithography, metal evaporation and lift-off process. The basic electrical transport properties and biological response of In_2O_3 nanowire device were also characterized.

Figure 1a shows the *I-V* curves of a typical In_2O_3 device with applying different gate-voltages. It was found that the device is significantly sensitive to electrostatic gating and the nanowire is working as n-type channel. This can be clearly observed in the I_{ds}-V_g curve shown in Figure 1b, where a change up to three orders in device conductance was observed when V_g was swept from -25 to +25V. Meanwhile, the *I-V* curves are found to be linear at low bias, which indicates the good ohmic contact formed between nanowire and metal electrodes. This is good to investigate the biological detection.

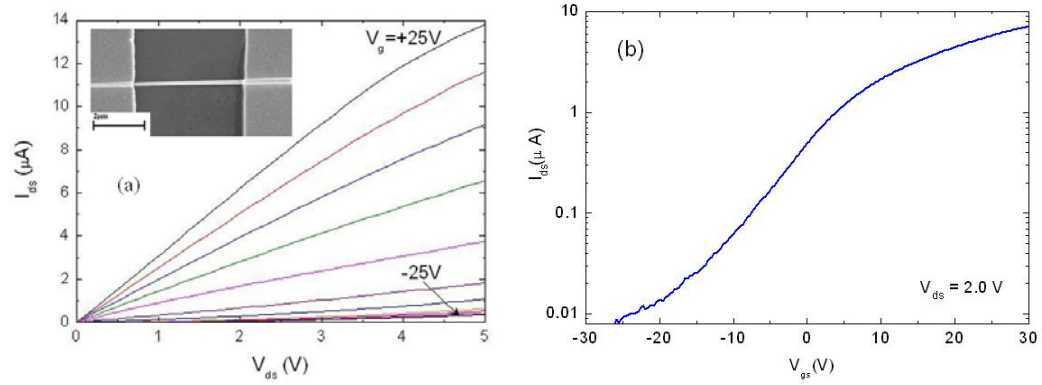

Fig. 1: (a) I-V curves of a typical In_2O_3 device with respect to back-gate voltage (V_g = from +25 to -25V with a step of 5V). The inset is the corresponding SEM image. (b) The corresponding I_{sd}-V_g curve at V_{sd} of 2.0V.

B. Microfluidic channel integration

The In_2O_3 FET devices were used to work as biological sensors. Firstly, PMMA was used to passivate the devices. The stability of the devices was investigated by measuring the conductance as a function of time (shown in Fig. 2). It can be seen that the conductivity of the nanowire is very sensitive to the environment, e. t., a peak in conductance appears once the noise is introduced. Therefore, the noise is a big obstacle for the stable and reliable measurement.

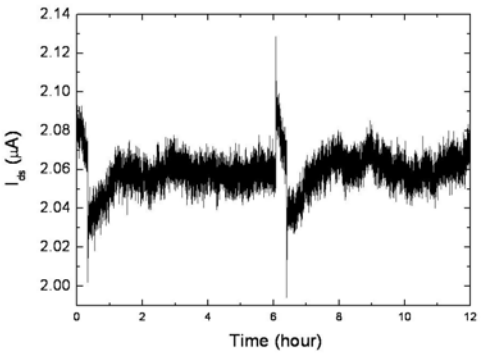

Fig. 2: Current-time dependence of a typical In_2O_3 device in dry air.

In order to resolve this noise issue, the microfluidic system is necessary to introduce into our measurement. Figure 3(left) shows a device integrated with microfluidic system. The two pipes and PDMS microchannel form a microfluidic system. After combined with microfluid channel, we investigated the basic electrical properties. Two devices show the FET properties, and others were broken during the integrated process. Figure 3 (right) shows the *I-V* curves of one device with applying different gate-voltages, indicating the nanowire is working as n-type channel.

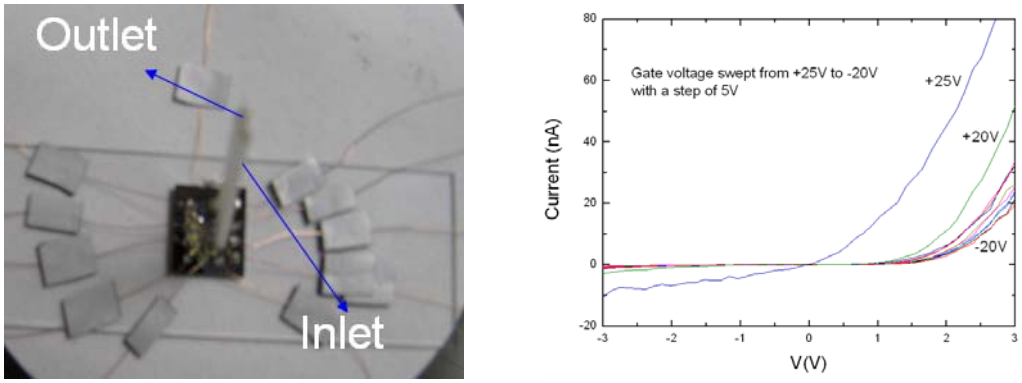

Fig. 3: (Left) SEM image of one chip device integrated with microfluid channel. (Right) I-V curves of one typical FET device with respect to back-gate voltage (V_g = from +25 to -20V with a step of 5V).

C. Biological detection study based on In_2O_3 nanowires

Initial biological tests of In_2O_3 FET devices were done by introducing biological solution through pipe. In order to repeatable test the reaction of the nanowire to surface bonded molecules, it is necessary to flow fluids across the nanowire surface in a precisely controlled manner. This step is also an important step for further development towards packaged, user-friendly sensors with integrated microfluidics.

We injected PBS buffer at 0.1M, and Ricin antibody and antigen (0.03mg/ml) into the microfluidic channel in sequence. Figure 4 shows the current-time curve when exposure to different solutions. It can be clearly found that PBS increased the conductivity of the nanowire. At first we hoped to inject PBS buffer into the channel to establish baseline conductivity. However, the conductance is unstable as shown in Figure 4. Although we observed the response of ricin antibody and antigen, it is not sure that the conductance change is really from the ricin at present.

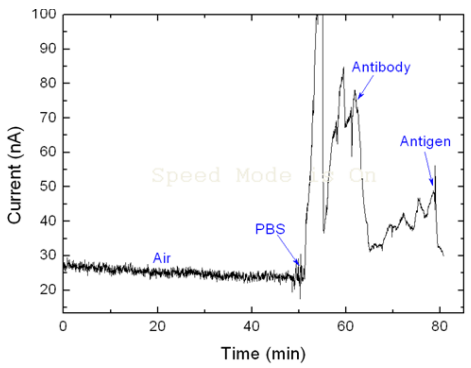

Fig. 4: PBS buffer, and biological response of an In_2O_3 device.

The reason for unstable conductance may be attributed to the poor passivation. In our experiment, we used PMMA to passivate the device, but PMMA layer may worsen when exposure to solution, and further affects the electrical properties. In the future, we'll employ metal insulator (for example, Si_3N_4) to passivate the device and do dynamic biological detection.

Ⅱ. Silicon Nanowire for biosensor application

The mechanism of nanowire sensors is based on carrier density changes when targeting molecules attach on the nanowires surface. Applying a gate voltage on the nanowire will simulate the carrier change process in the nanowire channels. So, the effect of gate voltage on the conductivity change of nanowire is an efficient benchmark on the sensitivity of nanowire based sensors. Up to now, most of nanowire based biosensors were fabricated through bottom-up method. However, this method suffers from certain limitations such as incompatibility with modern semiconductor manufacturing techniques and its large scale integration.

One solution is to utilize semiconductor processing techniques (top-down) to fabricate Si nanowire devices. The main advantage of this method is that the location of the nano-wires is now pre-determined by the lithography process and doesn't require 'manual' wire alignment.

Figure 5 illustrates the process of top-down approach, summarized as follows: i) Starting with silicon-on-insulator (SOI) wafer that consists of a 380nm buried oxide layer and a 100~280 nm silicon layer on insulator; ii) Cr mask fabrication by e-beam patterning, Cr metal deposition and liftoff process; iii) Silicon etching by a reactive ion etching system and Cr mask remove by Cr etching solution; iv) After that Ti/Au electrodes deposition by e-beam pattern, metal deposition and liftoff; v) Finally, depositing Si_3N_4 insulator layer to passivate the electrodes and exposing the Si nanowires.

In the process the e-beam lithography and the reactive ion etch are the key steps to obtain the Si nanowires with high quality. The former defines the nanowire size and the latter dominates the performance of this method. If the etching time is not enough, the Si layer would etch incompletely. In contrast the insulator layer (SiO_2) may remove partially, worsening the dielectric properties of nanowire devices. Initial etching conditions were using an ICP power of 600 W, an Rf power of 15W, and a pressure of 20mtorr with CF_4 as etch gas. The results are

shown in Figs.6 clearly stating that more process optimization is required to achieve smooth sidewalls of the channel/wire structures.

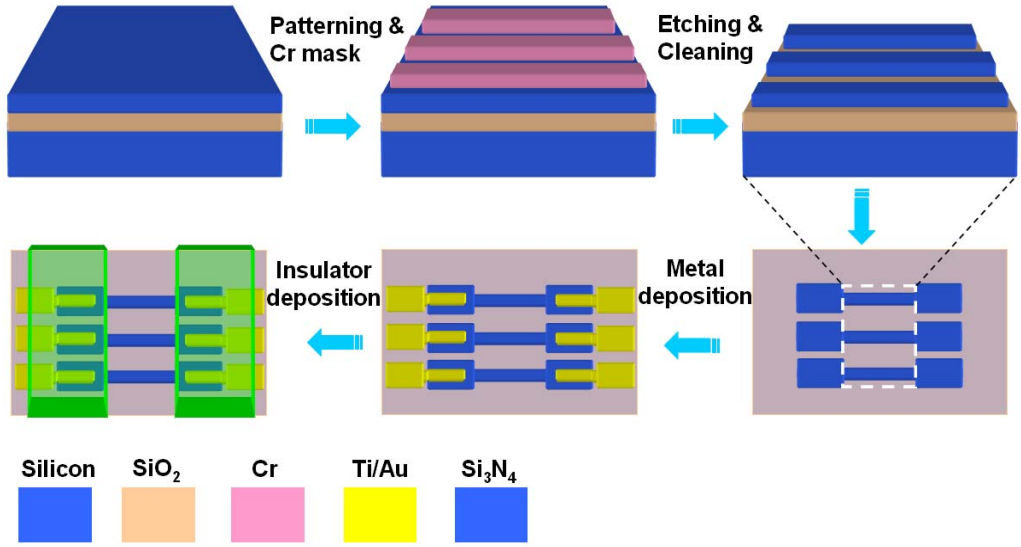

Fig. 5: Schematic diagram showing the Si nanowire device fabrication process through top-down method

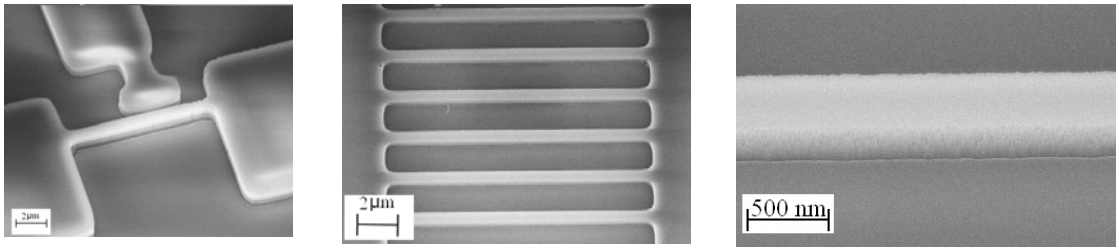

Fig. 6: Examples of etched nanowires and channels, the Cr layer was nearly etched away allowing the gas to attack the covered silicon layer and also partly the SiO_2 layer.

In order to enhance etch contrast between Au and Si/SiO_2 another Cr layer was added as well as leaving the e-beam resist on top of the metal layer for further protecting it from the etch gas. While using of Cr for a high-selectivity etch-mask layer, the etching conditions of ICP power and bias voltage could be enhanced to control the etch-rate and uniformity. Figure 7 (a) and (b) show the SEM image of single and double Si nanowire device with optimized process, the width and height of the Si nanowire is about 300nm and 280nm, respectively. Meanwhile, it can be seen that the Si nanowire has good shape. The basic electrical properties were investigated by measuring current (I)-voltage (V) curves as shown in Figure7 (c) and (d). I-V curves shows the Si nanodevices have good conductivity, indicating the Si nanodevices are suitable for biological detection.

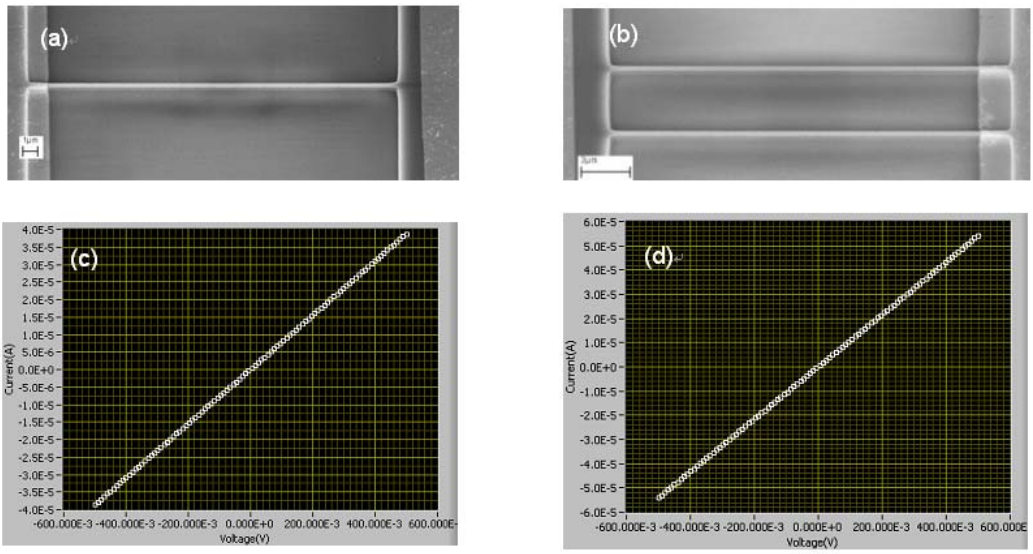

Fig.7: SEM image of single (a) and double (b) Si nanowire device, (c) and (d) are the corresponding current- voltage curves.

In preparation of using dies from different materials as sensor chip embedded into the fluidic stack different substrates have been shipped out for dicing and received back recently (Fig. 8). The initial metrology indicates that the tolerances of diced chips are tightly controlled and that integration of these chips with fluidic PMMA modules should yield similar results as achieved with glass dies so far.

Figs.

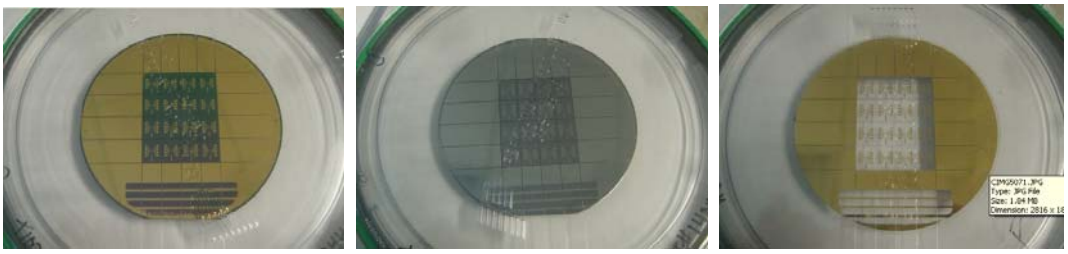

(a) (b) (c)

Fig. 8: Diced sensor chips from (a) SiO_2/Si wafer (b) SOI wafer (c) glass wafer.

Ⅲ. Microfluidic Engineering Research

A. Status last report and novel approach

Figure 9 illustrates the principle arrangement of the biosensor device. A Si-based nanowire electrode chip is sealed with a polymer fluidic cap which allows for introduction of sample fluid into the cavity. Through selective binding to molecules (Antigens) attached to the nanowires a change in electrical signal from the nanowire will be induced and allows registration of the presence of specific molecules in the sample.

The electrode pattern is covered with an insulating resist layer leaving only defined areas (mainly nanowire) of the electrode pattern accessible to fluids carrying biological samples across the electrode area. Figure 10 illustrates a basic experimental setup using PDMS caps with electrode test structures reported last year.

A number of limitations associated with the handling and interconnecting of silicon dies and polymer microfluidics resulted in a novel approach utilizing the microfluidic stack concept developed at CAMD. The overall concept is outlined in Fig. 10 and explained briefly in the text.

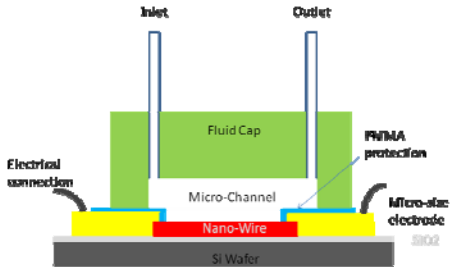

Fig. 9: Schematic of the sensor dye – polymer fluid cap assembly.

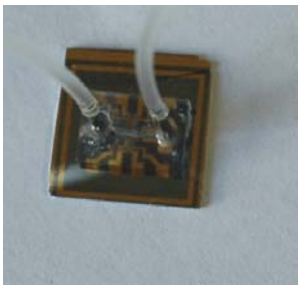

Fig. 10: Completely assembled die with fluidic cap and tube interconnects.

Ⅲ. Microfluidic Engineering Research

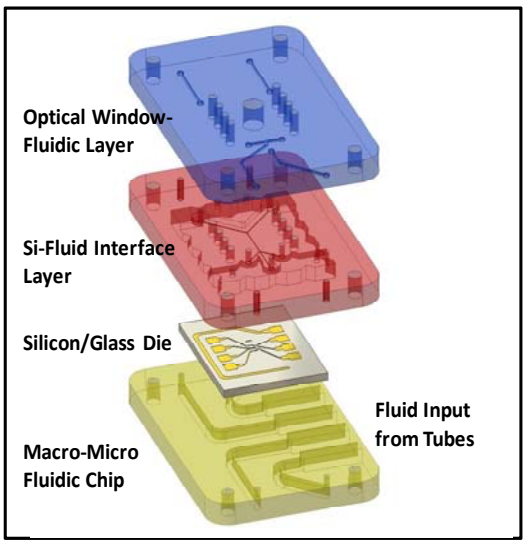

Fig. 11: exploded inventor model of impedance spectroscopy module, consisting of 3 PMMA modules containing fluidic structures and glass die with microelectrodes.

The sensor device is built from different polymer modules (outer dimensions are roughly 25mm x 15mm x 5mm) each performing specific functions or providing standardized interface feature. In particular the device is made from three PMMA modules is illustrated. Starting from the bottom chip (yellow module) fluids (up to 4 different solutions) can be injected into the stack using syringe pumps connected to flexible tubes. Four channels provide a well-defined position for steel-tubes that are glued into the chip and can be connected to external fluid media as needed. Within the yellow chip fluids are directed to different locations from where they flow up to the next level (red chip). The red chip is patterned on its bottom with a recess to accommodate the silicon or glass dies which contain microelectrodes (or electrodes with nanowires) as well as open microfluidic channel. There are an additional 6 holes to fill in conductive glue connecting to the bond pads of the Si dice. The fluidic microstructure is a simple, straight channel connected to one inlet and one outlet passing fluid across the electrode area. The stack is completed with the blue chip that has openings for the electrical connections (same as in the red module), an optical window (= hole to minimize the cap thickness for microscope inspection) and two fluidic channels connecting to the inlet/outlet of the red chip and also to the fluid outlets of the yellow

chip. A number of designs with different channel sizes were fabricated and also additional features like hydrodynamic focusing are implemented to enable controlled movement of the sample stream to the electrode pattern.

B. Microfabrication and Assembly Efforts

The modules containing the microfluidic channel structures were fabricated in biocompatible Polymethylmethacrylate (PMMA) sheets by polymer hot embossing on a Jenoptik® Mikrotechnik HEX02 machine. The master mold (see Fig. 12) was fabricated in brass from an AutoCAD® design by direct milling with a KERN® precision micromill. For embossing, the substrate was first was heated to 160°C, and then a pressure of 1.77MPa was applied to press the mold into the softened PMMA substrate. After cooling, the mold and substrate were separated leaving a channel pattern transferred into the PMMA. The chips were fly cut by a Precitech Optimum130 to a thickness of 1.5mm opening up fluidic vias and also removing material between adjacent chips, allowing easy separation of individual modules (Fig. 13).

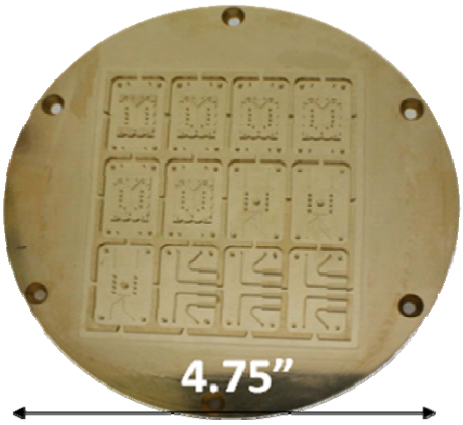

Fig. 12: Micro-machined brass mold inserts containing 12 different chip designs.

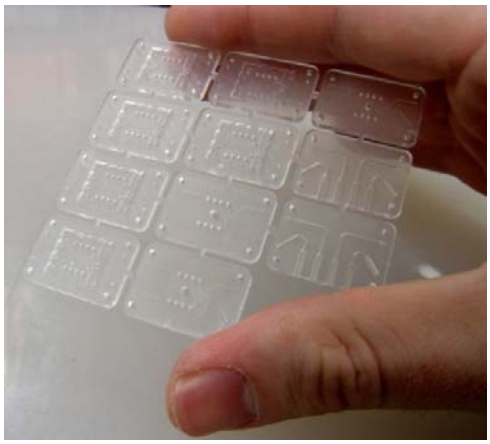

Fig. 13: Molded and fly-cut chips ready for assembly.

An optical UV-mask containing the original electrode array design was used to pattern microelectrodes onto a gold-coated silicon dioxide substrate using UV-lithography and wet-etching. The microelectrode patterns are patterned onto a 4” silicon wafer which is subsequently precision-diced to the format of the fluid module with an accuracy of ±25µm. (see also Fig. 14).

Prior to thermal bonding all three modules into a fully sealed stack additional assembly steps are performed. For example, steel tubes are cut to length (~2cm) and glued into the Macro/Micro interface module using UV-glue and flood exposure with UV-light (Oriel UV-lithography station). Another critical step is the exposure of the glass die and fluidic interface module to RF oxygen plasma at 100mW for 1 minute before fitting the die tightly into the cavity to enable leak-free sealing (see Fig. 15). To further enhance the bonding quality, a sheet from low molecular weight PMMA was cut to the size of the cavity/glass die and placed between the macro/micro - fluid interface chip and the glass chip. After completing assembly of all modules a thermal bonding process at a pressure of 0.5MPa for 2h at 104˚C, which is slightly below the glass transition point (Tg=105°C) of the PMMA modules was performed that resulted in a tightly sealed stack. Initially, surgical rubber tubes were bonded to the steel tubes in an effort to

strengthen the fluidic interconnects. However, this method didn't provide the necessary firmness. To overcome this issue, a septum was created by injecting silicone into the fluidic interconnections replacing the steel tubes. This way, small syringe needles can be used to leak-free inject the sample and buffer fluids into the stack. Figure 16 shows a fully packaged stack where Cu wires were glued into openings using a conductive glue that also established the electrical connection with the microelectrodes.

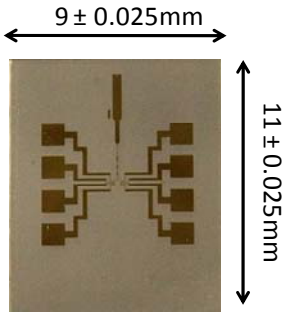

Fig. 14: Precision diced Au/Cr electrodes patterned on glass substrate.

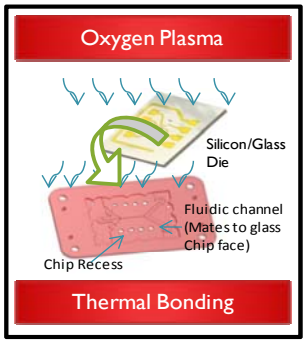

Fig. 15: Surface modification and assembly of die into the molded fluidic module.

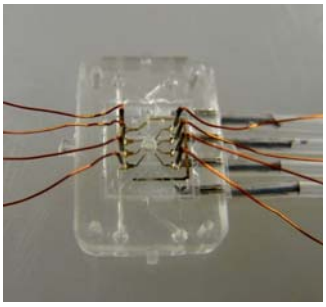

Fig. 16: assembled stack with glass die, fluidic and electrical interconnect structures to the outside world.

Taking advantage of the high precision microfabrication process employed to patterning the custom-designed PMMA module, Si or glass dies can be passively inserted into the recesses with minimal assembly efforts (passively aligned). On-chip alignment markers with dimensions of 20µm with 20µm gaps were patterned onto the glass chip, too to enable visual inspection after the assembly process was completed. Since the microfluidic channels were fabricated symmetrically to the z-axis comparing the position of the channel to position of alignment markers provides information about the alignment accuracy during the assembly process. Evaluating the information from the markers shown in Figs.17 illustrates that alignment accuracy of better than 15µm was routinely achieved.

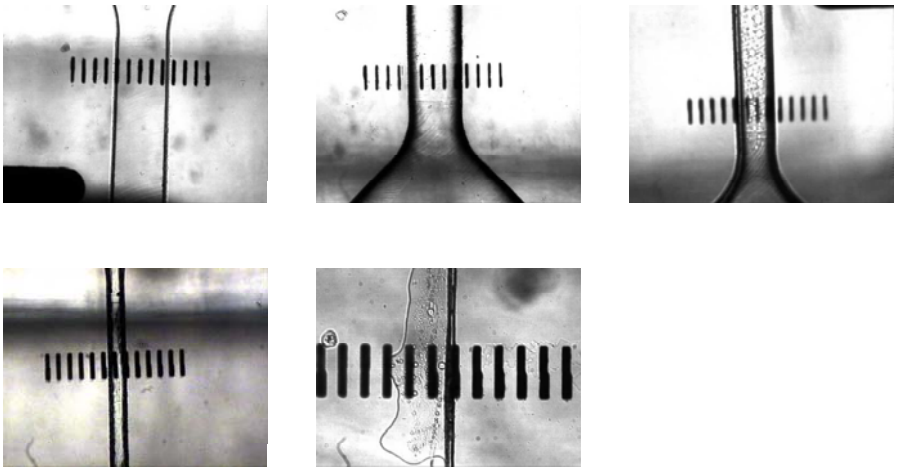

Figs. 17: Markers (~20 µm) from gold on glass die aligned to different channel sizes; from up left to down right: 200µm, 150µm, 100µm, 60µm, 20µm. Passive alignment yielded an accuracy of better then 15µm.

After optimizing process parameters excellent bond strength was achieved that allowed fluid testing using a dyed water fluid. Figures 18 show fluid flow through channels of different width past a microelectrode assembly. A study done by Han *et al.* [Han A et al (2003) "Multi-layer plastic/glass microfluidic systems containing electrical and mechanical functionality", Lab Chip 3:150–157] ascertained a maximal bond strength of 20kPa at a PMMA/Glass interface

Our bonding process yielded leak free channels up to fluid pressures of 83 kPa indicating an even better bond and superior performance of our fluidic package. In addition to simple fluidic structures an arrangement of microelectrodes was patterned that was used to optimize the electrical interconnection within the assembled stack.

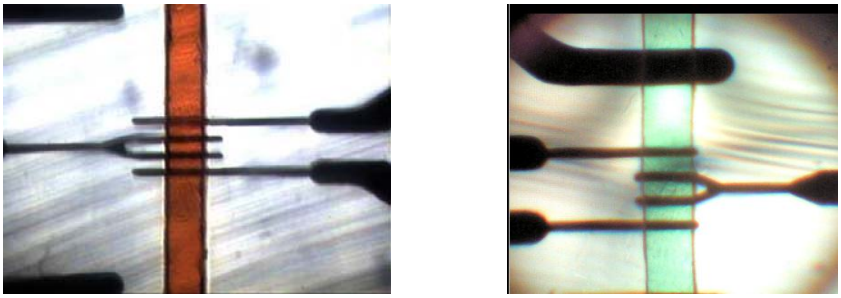

Fig. 18: Demonstration of leak-free PMMA/Glass interface with (a) red dyed water in a w=60µm, and (b) green dyed water in a w=200µm wide channel. The ensemble of four microelectrodes (~10um wide) interfaces the fluid and allows observation of fluid flow (see next chapter).

C. Initial Electrode Measurements

Using the configuration of four microelectrodes in a Wheatstone bridge configuration a potential difference between two sub-circuits can be measured allowing to analysis and evaluate the electrical interconnection. Two resistors (1MΩ each in order to reduce the settling time) were connected in series between excitation signal and measurement electrodes. Since this potential change is typcially very small and noisy, an amplification circuitry was designed and fabricated (PCB technology). As shown in the schematic (Fig. 19) the microfluidic sensor was connected to an off-chip fast settling instrumentation amplifier, which uses a differential amplifier to multiple the differences between the two sub-circuits with a high frequency bandwith. The instrumentation amplifier consists of three AD854JN with an adjustable gain configuration, giving an overall gain of 201 at 10MHz bandwidth. Since microfluidic channels interfacing with electrodes provide a high noise environment and the recorded/excitation-signal-ratio is approximately 1/1000 the signal had to be demodulated in order to eliminate noise by using an extreme band-pass filter. The amplified representation signal feeds a self-made lock-in amplifier circuitry which is connected to the function generator due to a unity gain buffer operational amplifier (LT1037).

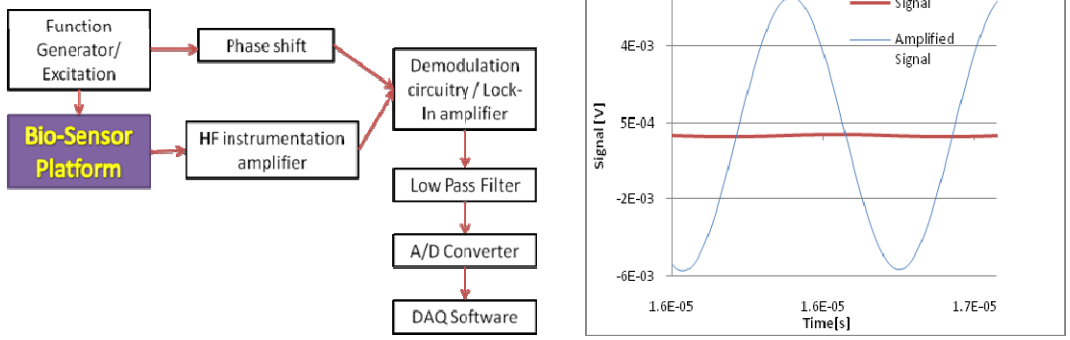

Fig. 19: (a) Block diagram of electronic circuitry (b)Magnitude of normal and amplified signal due to cell passing detector at 1MHz for 5µm cell in PBS (Multisim simulation).

Heart of the circuitry is a phase trim configuration in series with a comparator connected to the function generator and a LTC1043 capacitor switch configuration to demodulate the signal and sense small impedance changes (usually µV) in high-noise environments. INA114 based low-pass filters were added to minimize the noise and regulate the bandwidth.

Signals were acquired by an AD/Converter and MCC-DAQ-Software. First electrical measurements using air bubbles within a continuous flow of water to detect signal changes illustrate that the assembly was completed successfully and the detection scheme works (Fig. 20). These initial tests were performed by interfacing the assembly to NE-OEM application syringe pumps with 1ml BD plastic syringes to inject a dyed buffer fluid to perform visual leakage tests and connection the soldered copper wires and signal-processing electronics to a data acquisition program.

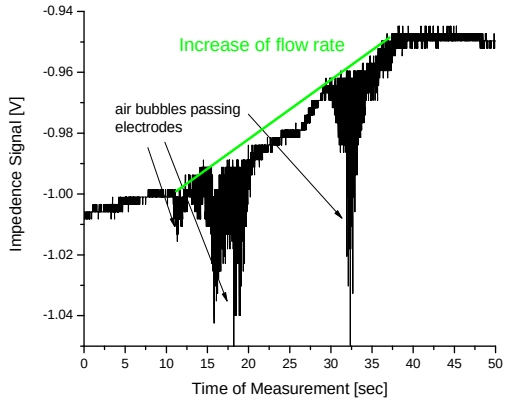

Fig. 20: Impedance measurement proving successful connection of electrodes within the stack.

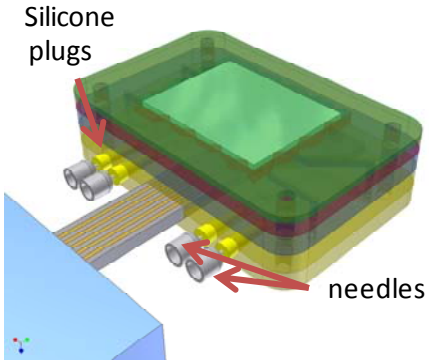

Fig. 21: Schematic of an advanced stack package using a customized PCB solution embedded into the stack and connected to an external circuit (blue box); fluid interconnects will be realized using a silicone septum and syringe needles for leak-free, simple interconnection of fluids.

D. Summary and Outlook

In the past year our efforts have been focused on designing and optimizing a stack based integration concept for silicon/glass die based sensing devices. Design, fabrication, and assembly have been successfully tested using microelectrode configurations interfacing with fluid transported through microchannels. The initial electrical tests indicate that more advanced electronic circuit design is needed in order to improve signal-to-noise ratio and enable reliable detection of electrical changes indicating a selective binding events of target molecules with engineered nanowires.

While our recent efforts are promising a number of details still need to be addressed and optimized, including:

- interface issues within the stack, in particular electrical interconnects and optimized electrical circuits; these efforts will focus on a customized printed circuit board (PCB) and methods to integrated them as additional module into the stack in order to minimize the length of the electrical interconnect (see Fig. 21);
- design of additional fluidic modules to support sample flow manipulation, esp. ensuring that the sample will be passed across the embedded nanowires;
- further explore the lithography based patterning of Si nanowires as an alternative approach to the manually attached nanowires; pursuing an all lithography based fabrication process will ensure wafer-scale fabrication and ultimately cost-effective fabrication of sensor devices.

Ⅳ. Genetically engineered antibodies for nanosensors

A. Brief Narrative

We are making genetically engineered antibodies that will bind to nanomaterials better than the native antibodies. Working with two different antibodies we have introduced three different Cterminal domains onto them, and expressed them as full length antibodies or Fab fragments. We have now demonstrated that an engineered antibody binds to unencapsulated quantum dots, whereas the wild type antibody does not. The bound antibody retains function and antigenic specificity. We have also devised methods to maintain these QDs in solution in the presence of physiologic salt solutions.

B. Objectives

We are making genetic modifications to antibodies to improve their utility in biosensors. These modifications should allow for greater coupling efficiency and for orientation of the antibodies with their binding sites exposed. Two different antibodies are being modified: 1. RAC18, an antibody to ricin toxin, a molecule of biodefense interest, and 2. anti-HIV antibody HY, directed to the virus envelope. For each antibody, we are attaching to the full length and Fab three different heavy chain carboxy-termini: 1. the metal binding 6X-His motif, 2. oligo-lysine (free amino groups), and 3. oligo-cysteine (sulfhydryl groups). We will compare the function of these 12 constructs with native Ig. They will be studied free in solution and bound to nanowires or quantum dots. We have made all four 6XHis constructs, and the four full-length oligo-lysine and oligo-cysteine constructs. Antibodies for each have been made and purified. We are conducting tests of the coupling of these antibodies to quantum dots and to proteins. Our studies of the binding of these molecules to nanowires have been delayed because the chemical

modification of the nanowires has not been completed. We demonstrate promising results showing the function of 6X-his modified antibodies when attached to quantum dots.

C. Research Progress

We have continued to work with QD-bound antibodies and demonstrated that they have functioned effectively for periods of up to one month post conjugation.

The majority of our efforts have been directed towards producing large quantities of theantibodies that we desire to study further. We currently are able to express 1-2 mg antibody/liter of tissue culture using transient transfection. We have been unable to identify stable transfectants producing meaningful quantities of antibody. To achieve higher expression levels we are using an expression system in which the expression is driven by transactivation via the Epstein-Barr Virus Nuclear Antigen and then by the SV40 T antigen. The antibody genes have been transferred to a plasmid containing the EBV Ori-P and transactivation domain. These will be transfected into 293 cells expression EBNA. This will maintain the plasmid as an episomal element. The cells can then be transduced with a retrovirus vector expressing SV40-T. This will drive plasmid replication (the plasmids encoding the antibodies also contain SV40-Ori) and should result in a massive increase in antibody production. We are currently selecting the cells containing the transfected plasmids.

V. Project 3 (Mark DeCoster - LA Tech). Patterning and characterization of nanowires integrated into a biochip detection device; Modification with linkers and tails for secreted phospholipase A_2 detection using LBL technology and biocompatibility assessment

1. Personnel

co-PI: Dr. M. Decoster; Undergraduates: Michelle Sibille, Enkhjin Bayarsaikhan, and Chris Chain; Master's level graduate students: Raj Masvekar, Jessica Wasserman, and Dustin Green; Ph.D. student: Jim McNamara provided significant research and training for the lab for this project.

2. Activities and Findings

Results- Testing of Nanomaterials toxicity to brain cells.

All cultures were exposed to nanomaterials for approximately 21 hours. MTT assay was then run to test culture activity. Results for MTT assays were read using spectroscopy set at 570nm. Figure 1 gives an indication that specific concentrations of Si nanoparticles may increase cell activity in astrocytes, without causing toxicity observed with copper nanoparticles. A similar curve is seen in figure 3 at the same concentrations. Aged nanomaterials tested in figure 2 suggest that allowing opper to oxidize may make it less reactive to the cells.

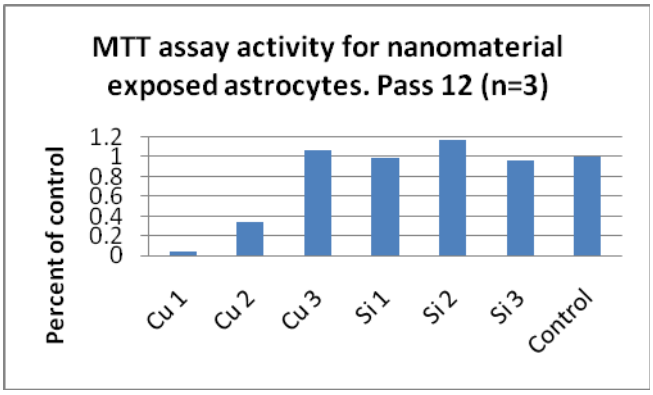

Figure 1. Pass 12 astrocytes exposed to nanomaterials. Astrocytes were taken from culture of rat brain astrocytes.

Cu 1= copper nanoparticles, 100µg/mL; Cu 2= 50µg/mL; Cu 3= 10µg/mL; Si 1= silica nanoparticles (UNO), 100µg/mL; Si 2= 50µg/mL; Si 3= 10µg/mL. Control = Locke's solution

- Describe the opportunities for faculty recruitment, retention and development, as well as post-doc, graduate and undergraduate student training provided by your project;

Undergraduates who were trained in the project: Michelle Sibille, Enkhjin Bayarsaikhan, and Chris Chain. Michelle Sibille has been accepted to medical school for fall 2009. Master's level graduate students: Raj Masvekar, Jessica Wasserman, and Dustin Green. Raj Masvekar and Dustin Green have been accepted into Ph.D. programs away from Tech for fall 2009 and Jessica Wasserman has been accepted into the Ph.D. program in Biomedical Engineering at Tech for Fall 2009. Post doc Dr. Mangilal Agarwal worked for the project for one year.

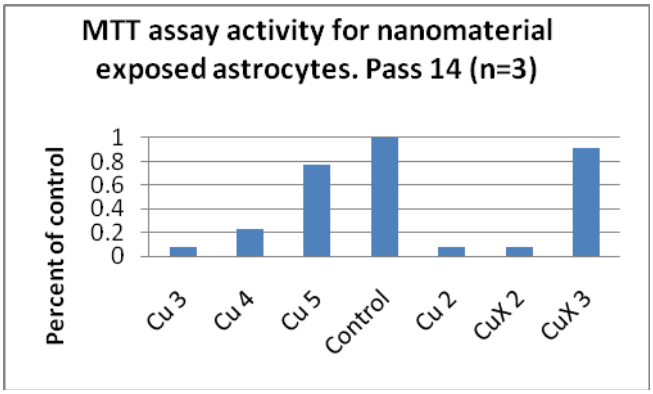

Figure 2. Pass 14 astrocytes exposed to fresh nanomaterials and some nanomaterials that had been aged for approximately one month in Locke's solution.

Cu 3= copper, 100µg/mL; Cu 4= 50µg/mL; Cu 5= 10µg/mL; CuX 2= 50µg/mL aged in Locke's solution for one month; CuX 3= 10µg/mL aged in Locke's solution for one month

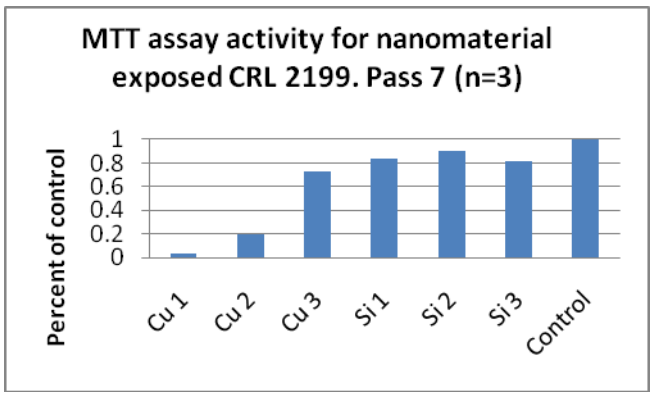

Figure 3. Pass 7 CRL 2199 type cancer cells exposed to nanomaterials.
Cu 1= copper, 100µg/mL; Cu 2= 50µg/mL; Cu 3= 10µg/mL; Si 1= silica nanoparticles (UNO), 100µg/mL; Si 2= 50µg/mL; Si 3= 10µg/mL. Control = Locke's solution.

- Describe the opportunities for faculty recruitment, retention and development, as well as post-doc, graduate and undergraduate student training provided by your project;

Undergraduates who were trained in the project: Michelle Sibille, Enkhjin Bayarsaikhan, and Chris Chain. Michelle Sibille has been accepted to medical school for fall 2009. Master's level graduate students: Raj Masvekar, Jessica Wasserman, and Dustin Green. Raj Masvekar and Dustin Green have been accepted into Ph.D. programs away from Tech for fall 2009 and Jessica Wasserman has been accepted into the Ph.D. program in Biomedical Engineering at Tech for Fall 2009. Post doc Dr. Mangilal Agarwal worked for the project for one year.

- Describe the nature and scope of partnership activities;

Drs. Lvov and Decoster –AMRI annual conference in February 2009, and discussed results with AMRI researchers. 2 joint reports were presented at AMRI Mardi Gra symposium. With Prof. Kevin Stokes, we are working on preparation of the project on clay nanotube smart nanocontainer for anticorrosion coating.
Describe any problems encountered during the last year of project activities. Second year funding was delayed for six months and money received in December 2008, therefore, again we will need extension till December 31, 2009.

3. Contributions: Summarize efforts made to build research and education capacity, secure external federal and private-sector funding, and ensure project sustainability over the long term.

1. "Clay Nanotubes for Controlled Release of Corrosion Inhibitors," NASA-EPSCOR LA BoR, pre-proposal, PI, $200,000, Jan 2010-Dec 2011.
2. "Clay Tubule Nanocontainer for Responsive Corrosion Protection," NSF-nanomanufacturing, PI, $270,000, Sept- 09- Aug 20012
3. 'Microfluidic Device for Directed Assembly of Nanoparticles and Polyelectrolytes on in situ Generated Templates," NSF-nanomanufacturing, PI, $280,000, Sept- 09- Aug 20012
4. "Materials Synthesis in Clay Nanotubes," PI, NSF, $340,000, Sept 2009- Aug 2012

5. “Clay Tubule Nanocontainer for Responsive Corrosion Protection,” NSF-nanomanufacturing, PI, $270,000, Sept 09- Aug 2012
6. ‘Collaborative Research: Microfluidic Device for Directed Assembly of Nanoparticles and Polyelectrolytes on in situ Generated Templates,” NSF-nanomanufacturing (with Virginia Tech), PI, $280,000, Sept- 09- Aug 20012
7. pre-proposal: “IGERT Multi-Scale Integration of Biomimetic Systems,” NSF, PI: M. Decoster, NSF, $2, Sept 2010- Aug 2015

4. Project Revision: Provide a listing of and explanation for any significant changes in the work plan for upcoming year, including any changes in the amount of investigators' time devoted to the project. – Dr. Despina Davis replaced as co-PI Kody Varahramyan with responsibility for the first project

Publications

“Detection of H_2S at room temperature by using individual indium oxide nanowire transistor”, Zhongming Zeng, Kai Wang, Zengxing Zhang, Jiajun Chen, and Weilie Zhou, Nanotechnology **19**, 225303 (2008).

“Synthesis of Magnetic Porous Hollow Silica Nanotubes for Drug Delivery,” H. Ma; J. Tarr, M. A. DeCoster; J. McNamara; D. Caruntu; J.F. Chen; C. J. O’Connor; W. Zhou, J. Applied Physics, v.105, 981, 2009.

Presentations

AMRI DARPA review presentation “Field effect transistor for Antigen detection” Weilie Zhou and Seth Pincus (2009).

Q. Xing, S.Chen, M. DeCoster Y. Lvov, “Porous 3D Cellulose Fiber Based Microscaffold for Cell Culture,” TERMIS-NA 2008 (Annual Conference of Tissue Engineering & Regenerative Medicine International Society), San Diego, Dec 10, 2008.

J. McNamara, M. Decoster, Society for Biomaterials conference in San Antonio, Texas April 25, 2009. “Characterization of Micro-Patterned Templates for Promoting Spatially Defined Attachment and Growth of Neuronal Cells”.

M. Decoster American Society for Cell Biology, annual meeting in San Francisco, California, December 5, 2008. “Selective Adhesion and Growth of Astrocytes and Gliomas on Microscale Patterns Using Novel Molecular Printing Techniques”.

M. Sibille, J. McNamara, M. Decoster, Biomedical Engineering Society Meeting, St. Louis, Missouri, October 22, 2008. “CNS Glial Injury and Inflammatory Response in Normal and Cancer Cells”.

J. McNamara, M. Decoster, Conference on Magnetism and Magnetic Materials, Austin, Texas, November 12, 2008. “Synthesis of Magnetic Porous Hollow Silica Nanotubes for Drug Delivery”.

PKSFI Report for LEQSF(2007-12)-ENH-PKSFI-PRS-04

John Wiley
(PKSFI FRG-2, 2008-2009)

FRG-2 Nanomechanical Devices

1. Personnel:

This focused research group consists of researchers from the University of New Orleans (UNO) and Tulane University (TU). The principal investigators are John Wiley (UNO), Bruce Gibb (UNO), Scott Whittenburg (UNO), Leonard Spinu (UNO), Vijay John (TU), and Hank Ashbaugh (TU). A number of graduate students are also contributing to the work: Jianxia Zhang (UNO), Haiying Gan (UNO), Ovidiu C. Trusca (UNO), Joy St. Dennis (TU), Bhanukiran Sunkara (TU), Piyush Wanjari (TU), and Ashish Sangwai (TU). In one project, photoactive polymers are being synthesized and tested as possible light driven actuators in mechanical devices (Zhang in Wiley's group). In another project, sets of host-guest molecules are being synthesized and characterized as possible tethers for the directed self-assembly of nanocomponents (Gan in the Gibb's group). New magnetically guided tubular liposomes have also been produced for potential mechanical device components (Joy St. Dennis and Bhanukiran Sunkara in V. John's group; these researchers are working with Leonard Spinu in the characterization of these materials). Both the Ashbaugh and Whittenburg groups have been modeling various properties of host-guest systems. Ashbaugh's group (Piyush Wanjari and Ashish Sangwai) is studying mixed solvent effects on solvent-mediated interactions between hydrophobic species and Whittenburg is studying Brownian dynamics simulations of host-guest interactions as well as micromagnetic simulation of the nanoparticles. The latter project involves joint project between Whittenburg, Spinu and Trusca.

2. Activities and Findings:

The activities and findings will be broken up into the various aspects of the program.

a. *Photoactive polymers.* We are continuing our efforts to investigate the potential use of diazobenzene polymers for optically-active and solvent-active actuators. The polymers that we made last year have now been formed into nano- and micron-sized wires (Figure 2-1). We are currently examining both the effects of UV and solvent exposure on these wires. Individual micron wires have been dispersed and their optical response examined; while there are some bending in the wires, it is not as dramatic as what is seen in polymer films. We are currently looking to prepare asymmetric micron wires to see if we can influence the bending properties of these systems. We have also worked to disperse individual

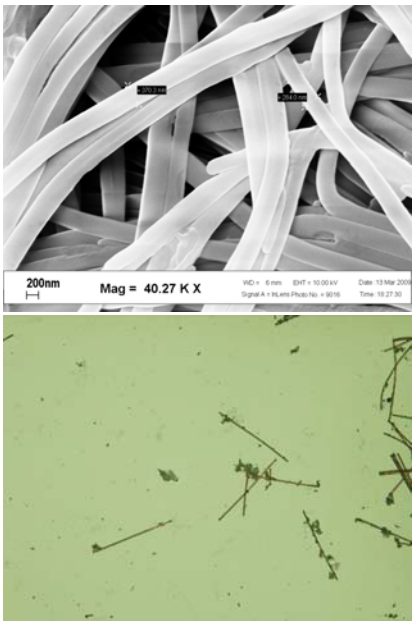

Figure 2-1. Diazobenzene wires. Top – SEM of nanowires. Bottom – optical micrograph of micron-sized wires

nanowires. We have a new scanning probe microscope on order that will allow us to monitor individual wires while they are exposed to UV light or different solvents. We hope to begin these experiments by mid-summer.

b. *Host-guest assembly.* This program of research focuses on the controlled assembly of nano-objects into complex nano-systems. The general approach involves the development of hosts (H1, H2 and H3) that bind complementary guests (G1, G2 and G3). Each host-guest pair is orthogonal, i.e. H1-G1 strongly associates, but for example H1-G2 or H3-G1 do not. Hence, one surface of a nano-object coated with H1 will stick to another object coated with G1. Moreover, with three, orthogonal host-guest pairs, it is theoretically possible to assemble complex objects by selectively coating different objects (or different parts of objects) with different hosts and guests. Our strategy is to utilize thioether-functionalized deep-cavity cavitand hosts (DCC) and complementary guests that bind strongly to gold surfaces.

The design of the hosts **1** and **2** (below) was based on work reported by Reinhoudt for a smaller host.[1] Of importance is the choice of thioether feet for the DCC over long chain thiols. Reinhoudt has reported that better surface coverage is obtained using the thioether feet since they are able to fold back under the resorcinarene head group upon binding of the sulphur atom to the gold surface to more effectively pack the space under the receptor. This results in a densely packed, more organized monolayer that passivates the gold surface better.[2] Hosts **1** and **2** have been synthesized following Reinhoudt's procedure.

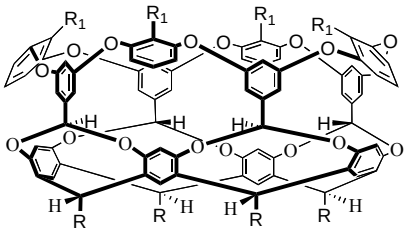

1: R = $(CH_2)_{10}S(CH_2)_9CH_3$, R_1 = H
2: R = $(CH_2)_{10}S(CH_2)_9CH_3$, R_1 = CH_3

The corresponding hosts for **1** and **3** (**3** and **4** respectively), have also been synthesized.

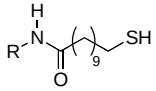

3: R = 1-adamantane
4: R = cyclopentyl

Since the last annual report, we have been focusing on synthesis of guest **3** coated gold nanoparticles.[3] We have synthesized three generations of this type of gold nanoparticles (**5-7**). NMR titration studies have been carried out using a (easily synthesized) model host with an identical cavity volume as **1**. No binding could be observed by this approach. To possibilities as to why this is the case are: 1) Insufficient solubility of the gold nanoparticles in DMSO (the best solvent for this type of study). 2) A very dense coating of guest molecule on the gold surface, which inhibited host complexation. In order to solve those problems, we designed **6** and **7**. In both of these entities, long carbon chain thiol that function as spacers were incorporated into the particle to increase the accessibility of the binding (guest) groups. In 7, these spacer groups were terminated with hydroxy groups to make the particles more

soluble in polar solvents such as DMSO. We have not completed the binding studies with these particles. These will include NMR studies, as well as TEM experiments.

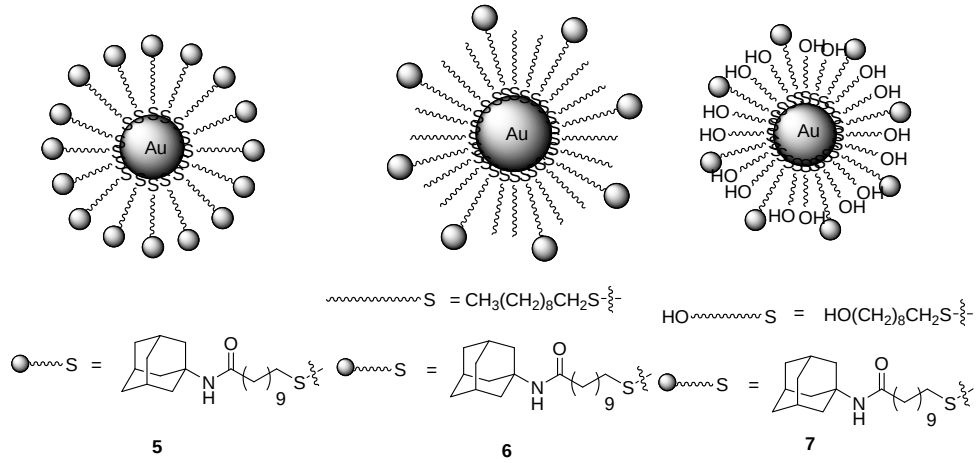

c. *Modeling of Host-Guest systems.* Over the past reporting period, research in the Ashbaugh lab has focused on calculating forces between cavitand hosts and adamantane guests in solvents of varying polarity. The molecular dynamics packages GROMACS was used in these calculations and simulations were performed on the LONI network. Umbrella sampling with weighted histogram analysis was used to evaluate the potential of mean force between the guest and host along the symmetry axis of the cavitand. Figure 2-2 shows a snapshot of adamantane adsorbed in the cavitand's hydrophobic pocket in water (water's not shown for clarity). Also shown is the potential of mean force evaluated in pure water and a 20 mol% mixture of ethanol in water. This plot shows that as the polarity of the solvent is decreased the attractive well depth decreases, indicating a reduced affinity for of adamantane for the cavitand. Ongoing research is examining a series of seven solvent mixtures studied experimentally by the Gibb group (UNO) to explain the observed binding affinity trends.

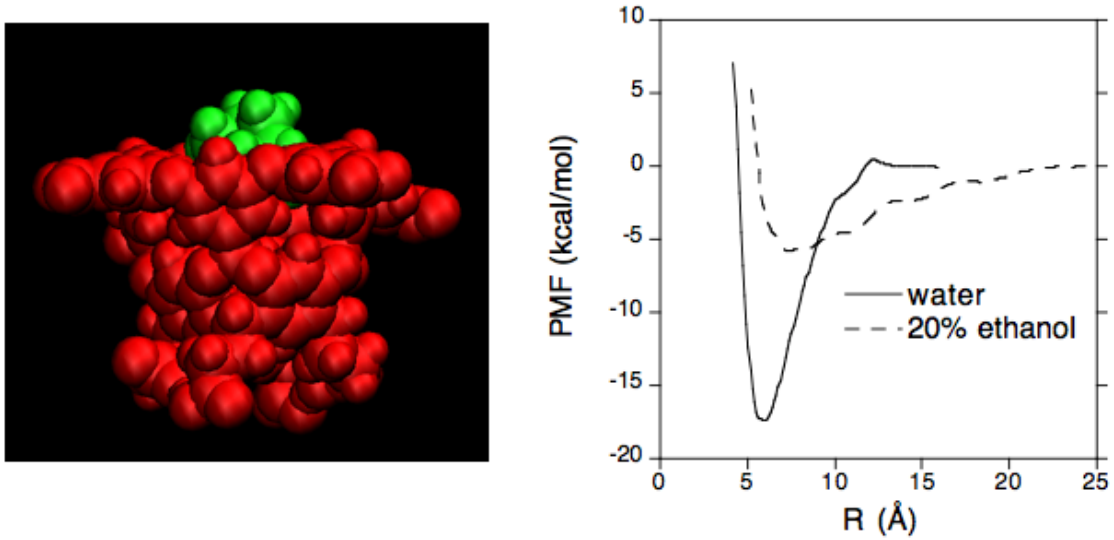

Figure 2-2. Snapshot of adamantane (green) tucked away into a cavitand (red) in water (left-hand figure). Potential of mean force for adsorbing adamantane into a cavitand in water and a 20 mol% ethanol – water mixture (right-hand figure).

In Prof. Whittenburg's efforts in the study of the Brownian Dynamics (BD) of the host-guest systems, he has worked to move his BD computer code to the LONI supercomputers. He has successfully compiled the code and has used it to conduct simulations on the binding of hydrogen bromide (as simple test case) to deep-cavity cavitands. The experimental work on this binding studies is done in collaboration with co-PI Gibb. Whittenburg has also written programs to enable visualization of the resulting BD trajectories. The next step involves adding the magnetic force field from his micromagnetics code to allow simulation of the three-dimensional controlled ordering of nanometer-sized structures. The magnetic phase of this work is being done in collaboration with Spinu.

d. *Magnetically guided tubular liposomes.* A dual-lipid liposome system consisting of a phospholipid and a skin ceramide extruded though a 100 nm membrane yields novel tubular and helical liposomes. These liposomes were used as templates to generate highly aspherical silica nanocapsules with length to diameter aspect ratios exceeding 10. Many of these nanocapsules have the morphology of a bulbous end attached to a long tip, mimicking microneedles attached to a reservoir. The fidelity of helical liposomes is transcribed to the silicas and the long tips indicate helically entwined left-handed silica structures. The silica coating is expected to protect and stabilize the internal contents of the liposomes, as well as enable surface functionalization for applications in drug or targeted delivery.

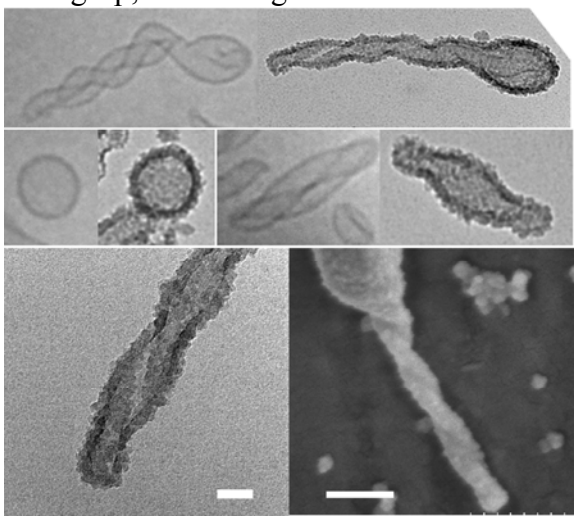

This work is a variation from the general liposome literature that is usually focused on spherical liposomes. Since recent literature highlights the importance of particle shape influencing clearance of particles from the body, we are interested in forming aspherical liposomes and extending the work to templation of such liposomes. We believe the liposomes especially those with high aspect ratio is interesting as the different shapes may give rise to non-conventional dissolution profiles. In the study, we show that liposomes composed of *L*-α-phosphatidylcholine and ceramide VI can be transcribed to form highly aspherical silica nanoshells with thin walls of 10 nm, while preserving the unique undulating feature of the liposomes. It is potentially possible to extend the technique to effect controlled release of the encapsulated liposome contents by an external stimulus e.g. infrared radiation or pH. In continuing research we are entrapping magnetic nanoparticles into these ceramized liposomes to form magnetically guided liposomal systems.

All of these projects offer extensive opportunities for the training of students and postdocs. Further, all the faculty involved in the project have greater opportunities for collaboration, beyond that outlined above, and this will lead to greater efforts in faculty retention as well as opportunities for successfully securing of joint funding. The success demonstrated by this faculty will serve to attract other highly motivated scientists and engineers to the New Orleans area.

The nature and scope of these projects are outlined above.

There have been no problems encountered over the last year.

3. Contributions:

Initially the focus was on building the research group, attracting students, initiating the research, and building the collaborations. This is now well established. Further efforts have gone to the purchase of a new scanning probe microscope from funding secured through the LA BOR Enhancement program by some of the PI's (Wiley, Gibb, Spinu); this instrument will serve several aspects of this program. In other cases (V. John), aspects of this project have been promoted to NASA, Sandia Laboratories and Los Alamos Laboratories where agencies are examining application potential.

4. Project Revision:

None

5. Work Products:

Presentations

"Fabrication of photosensitive polymer nanowires," Jianxia Zhang, Jin-Hee Lim and John B. Wiley, 235th American Chemical Society National Meeting, New Orleans, LA, April 6-10, 2008.

"Carbons from sugars: Morphology, microstructure and applications to gas storage," J. E. St.Dennis, Pradeep Venkataraman, Vijay T. John, Gary McPherson, Jibao He, Camille Y. Jones, Stephen J. Obrey, and Robert P. Currier, 235th American Chemical Society National Meeting, New Orleans, LA, April 6-10, 2008.

Effects of magnetic interactions in Ni nanowire arrangements Ovidiu Trusca, Dorin Cimpoesu, Jin-Hee Lim, John B. Wiley, and Leonard Spinu, APS March meeting, New Orleans, March 10-14, 2008.

"Interaction effects in Ni nanowire arrays," Leonard Spinu, Intermag Conference, Madrid, Spain, May 4-8, 2008

"Solvomechanical Response of Diazobenzene Polymer Films in Organic Solvents," Jianxia Zhang and John B. Wiley, Materials Research Society Meeting, Boston, MA, December 1 - 4, 2008.

Publications:

"Interaction effects in Ni nanowire arrays," Ovidiu C. Trusca, Dorin Cimpoesu, Jin-Hee Lim,

Xiequn Zhang, John B. Wiley, Andrei Diaconu, Ioan Dumitru, A. Stancu, and L. Spinu, *IEEE Transactions on Magnetics* **2008**, *11*, 2730.

"Shear Induced Formation of Patterned Porous Titania with Applications to Photocatalysis", Li, X.; John, V.T.; He, G.; Zhan, J.; Tan, G.; McPherson, G.; He, J.; Bose, A.; Sarkar, J. *Langmuir*, in press.

"Undulating tubular liposomes through incorporation of a ceramide into phospholipid bilayers", Xu, P.; Tan, G.; Zhou, J.; He, J.; Lawson, L.; McPherson, G.; John, V. *Langmuir*, in press.

"Bending Behavior of Polymer Films in Strongly Interacting Solvents," Jianxia Zhang and John B. Wiley, *Mater. Res. Soc. Symp. Proc.* **2009**, *1129*, 1129-V04-05.

PKSFI Report for LEQSF(2007-12)-ENH-PKSFI-PRS-04

Kevin L. Stokes
(PKSFI FRG-3, 2008-2009)

FRG-3: Nanomaterials for Energy Conversion and Storage

1. Personnel:

LATech/IfM

Abdullayev, Elshad. Graduate Research Assistant, Hydrogen storage materials
Agarwal, Mangilal. Laboratory Coordinator, Thermoelectrics
Carbo, Daniel. Undergraduate Research Assistant, Hydrogen storage materials
Davis, Despina. Co-PI, Thermoelectrics
Lvov, Yuri. Co-PI, Hydrogen storage materials
Mannam, Raja. Graduate Research Assistant, Thermoelectrics
Roy, Amitava. Graduate Research Assistant, Thermoelectrics
Singh, Varshni. Graduate Research Assistant, Thermoelectrics

LSU

Champagne, Chris. Undergraduate Research Assistant, Thermoelectrics
Karki, Amar. Graduate Research Assistant, Thermoelectrics
Walker, Nick, Undergraduate Research Assistant, Thermoelectrics
Young, David P. Co-PI, Thermoelectrics

UNO/AMRI

Gabrisch, Heike. Co-PI, Battery materials
Malkinski, Leszek. Co-PI, Ferroic composites
Mohanty, Debasish. Graduate Research Assistant, Battery materials
Nolting, Westly, Undergraduate Research Assistant, Thermoelectrics
Stokes, Kevin L. Co-PI, UThermoelectrics
Swart, Donald. Graduate Research Assistant, Thermoelectrics

Dr. Kevin Stokes reviews quarterly progress reports from LSU and La Tech to ensure that these contributions are adequate to the project's requirements.

2. Activities and Findings

A. Major Research and Educational Activities Undertaken

This focused research group (FRG) is applying the science and engineering of nanometer-scale materials to several areas of energy conversion and storage. Stokes, Davis and Young are investigating various aspects of nanocomposites thermoelectric materials and microdevices, Gabrisch is investigating novel electrode materials for electrochemical storage applications (rechargeable batteries); Malkinski is researching novel magnetic to electrical power conversion composites for micropower applications and Lvov is developing techniques for the nanoassembly of nanoparticles and tubule nanocontainers for possible hydrogen storage applications. There are six principle investigators, one senior researcher, seven graduate students

(total) and four undergraduate students from the University of New Orleans, Louisiana State University and Louisiana Tech. The results for June 2008 to June 2009 are summarized below.

B. Major Findings and Results

a. Electrodeposition of bismuth telluride (Davis)

This project aims to fabricate high quality TE nanomaterials (bismuth telluride nanotubes and nanowires) and to improve the Seebeck coefficient (power factor) by nanofabrication. The plan is to use complex pulsed electrodeposition techniques to make multilayered metallic and semiconductor nanotubes and nanowires. This unique (magnetic-thermoelectric) nano-architecture is not trivial to control, therefore complex, multipulse/pulse-reverse electrodeposition techniques will be explored and implemented. Using electrodeposition, a cost efficient and highly controllable method to fabricate Bi_2Te_3 nanotube and nanowires, it is possible to tailor the main carrier type in the alloy and to obtain either n-type or p-type semiconductors.

In this project different size nanotubes and nanowires of thermoelectric material Bi_2Te_3 will be synthesized inside the nanoporous polycarbonate (PC) and AAO membranes using electrodeposition. The plan is to study the effect of electrolyte composition and concentration on the resulting nanotubes Seebeck coefficients (thermo power). The plan is to evaluate the membrane pore diameters (resulting tube/wire sizes) effect of Seebeck coefficient values. Finally, a thermoelectric cooling device will be electrodeposited on a single membrane supporting the bismuth rich (p-type) and tellurium rich (n-type) nanostructures. Seebeck coefficient is one the key parameters that could be improved in large aspect ration nanotube/nanowire geometry and could lead to a higher thermoelectric power. Nanowires of bismuth-telluride Bi_2Te_3 are ideal thermoelectric materials because of their low thermal conductivity and high Seebeck coefficient.

Bismuth telluride (Bi_xTe_y) nanowires were electrodeposited from aqueous acidic solutions containing different $Bi^{3+}/HTeO_2^+$ (20/20 mM, 20/10 mM) concentration ratios. The polarization plots predicted that combined solutions exhibit more noble reduction potentials than individual solutions. Optimized deposition potentials were obtained from the combined electrolyte polarization plots. An anomalous codeposition behavior caused increase in Te concentration for depositions in the kinetic region of bismuth telluride; otherwise decreasing Te concentrations with increased deposition potentials was observed from composition analysis. X-ray diffraction showed a dominant (110) orientation for nanowires at low deposition potentials. N-type nanowires were obtained from both electrolytes, while p-type nanowires were only obtained from the 20/10 electrolyte for low Te (< 30%) concentrations. An intrinsic to extrinsic transition was observed for nanowires deposited from 20/10 electrolyte. The highest measured Seebeck coefficient was -318.7 μV/K and 117 μV/K for n-type and p-type nanowires, respectively. The Seebeck coefficient dependence on resistivity and composition of the nanowires is discussed.

Figure 1 shows the polarization behavior of the two studied combined electrolytes the 20/20, the 20/10, and their individual counterparts. Figure 1a illustrates the overall current profile of the 20/20 combined electrolyte, in which two distinct mass transport regions could be identified corresponding to the bismuth and tellurium components. From the partial current profiles the bismuth limiting current was reached at -150 mV. The overall current profile in the 20/20 combined electrolyte shows a shift toward the more noble potential region. Figure 1b shows the overall current of the 20/10 electrolyte and their partial currents. In this case the

individual tellurium limiting current was observed at -250 mV. The overall current profile in the 20/10 case maintained the same behavioral trend as the 20/20 electrolyte, noticing a negative shift in limiting current potentials.

The current behavior in the 20 mM Bi^{3+} individual solution showed a limiting value of -29 mA/cm^2 at -150 mV. In the individual electrolyte solutions, the $HTeO_2^+$ component limiting current was observed for low concentrations indicating a diffusion effect. For 20 mM $HTeO_2^+$ no clear limiting current was observed, while a limiting current density of -20.6 mA/cm^2 was observed at -250 mV for 10 mM $HTeO_2^+$. The equilibrium reduction potential of the combined electrolyte was found to be more

positive compared to the individual electrolytes due to the mutually induced codeposition mechanism. [24, 26] Addition of Te in the combined electrolyte shifted reduction potentials to more positive region. For instance, the reduction potential for combined electrolyte with 10 mM $HTeO_2^+$ plus 20mM Bi^{3+} (20/20) starts at 19 mV, while for 20 mM $HTeO_2^+$ plus 20mM Bi^{3+} (20/10) electrolyte starts at 34 mV. To be noted that the current in the combined electrolytes follows a similar trend in Bi^{3+} individual electrolyte. A limiting current was observed in the combined electrolyte when the individual kinetic region Bi current is less than the Te counterpart.

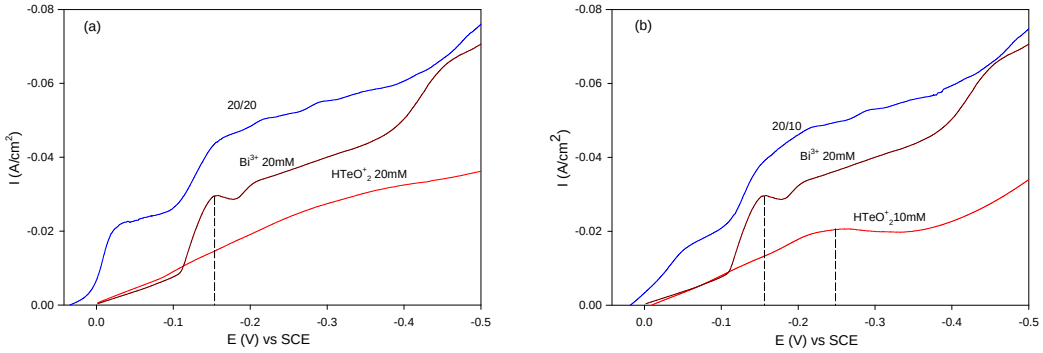

Figure 1a. Polarization curves of $HTeO^+_2$ (20Mm), Bi^{3+} (20mM), combined (20/20) electrolytes at a scan rate of 5 mV/s. Figure 1b. Polarization curves of $HTeO^+_2$ (10Mm), Bi^{3+} (20mM), combined (20/10) electrolytes at a scan rate of 5 mV/s.

Figure 2 shows XRD pattern of the nanowires deposited in AAO membrane at potentials -5 mV, -100 mV, and -300 mV from the 20/20 electrolyte. The nanowires deposited at -5 mV and -100 mV show a preferential (110) orientation, indicating that nanowires are polycrystalline with c-axis almost parallel to the nanowire length. However, the intensity of (110) peak decreased for nanowires deposited at higher overpotentials (-100 mV) and the (110) peak was strongly diminished for the sample deposited at even higher overpotential (-300 mV). Crystallite size calculations using the Scherer equation in JADE™ showed crystallite sizes of 210 Å, 150 Å, and 950 Å for nanowires deposited at -5 mV, -100 mV, and -300 mV, respectively. The XRD data suggests that the crystallite size is directly proportional to the deposition potential; higher the deposition potential larger the crystallite size.

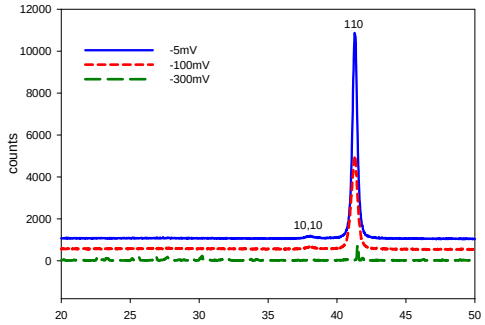

Figure 2. XRD of Bi_xTe_y nanowires deposited in AAO membranes at different potentials from 20/20 electrolyte.

b. Nanoparticle Composites (Stokes, Swart, Nolting)

We have prepared nanostructured Bi_2Te_3 and $Bi_{0.5}Sb_{1.5}Te_3$ powders. Briefly, elemental constituents (bismuth, tellurium and antimony) are loaded into a stainless-steel vial with stainless steel balls. The elements were purchased from ESPI; all elemental metals were 5N pure. We optimized the synthetic protocol by varying the length of ball-milling time as well as the ratio of the mass of the steel balls to mass of constituent material. We were able to obtain pure phases of both Bi_2Te_3 and $Bi_{0.5}Sb_{1.5}Te_3$. Figure 1 shows the powder x-ray diffractograms of the two compounds. Optimum conditions to obtain phase-pure samples were a ball-to- material ratio of 10:1 and ball-milling times of 25 to 40 hrs. Phase evolution was monitored at intermediate time intervals to establish the ball-milling protocols.

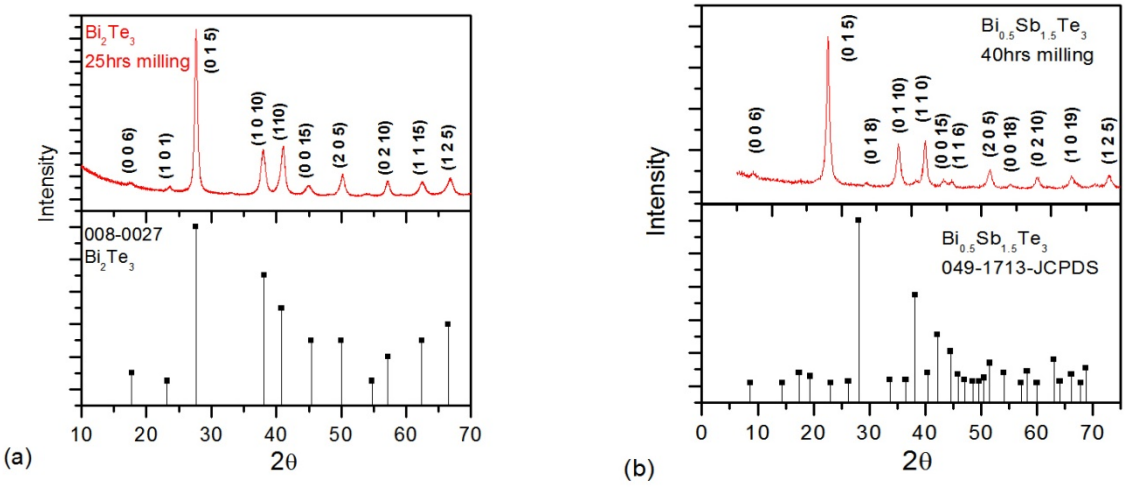

Fig. 1. X-ray diffraction patterns of (a) bismuth telluride and (b) bismuth antimony telluride powder samples. A comparison to Joint Committee on Powder Diffraction Standards (JCPDS) data is given in the lower graphs.

A representative scanning electron microscope (SEM) image of the ball-milled powders is shown in Fig. 2. The powders consist of large particles, on the order of several hundred microns. However, each large particle is an agglomeration of much smaller, nanometer-sized grains. These smaller, nanoscale structures are evident in the transmission electron microscope (TEM) image of the same powder shown in Fig. 3.

We have begun a preliminary study of the thermoelectric properties of these composites. The powders were consolidated in a uniaxial hot press. We were able to produce high-density pellets, 10 mm in diameter of both Bi_2Te_3 and $Bi_{0.5}Sb_{1.5}Te_3$. The density of the $Bi_{0.5}Sb_{1.5}Te_3$ sample was found to be 6.6 g/cm^3. This consistent with the density of the bulk alloy: The density of pure Bi_2Te_3 is 7.7 g/cm^3 and that of Sb_2Te_3 is 6.5 g/cm^3. A photograph of one of the pellets is shown in Fig. 4.

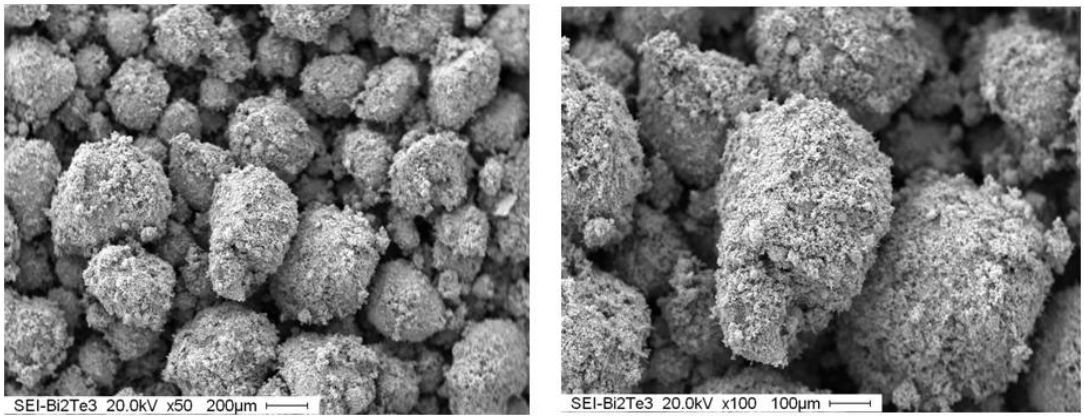

Fig. 2 Scanning electron micrographs (SEM) images of the ball-milled bismuth telluride powder.

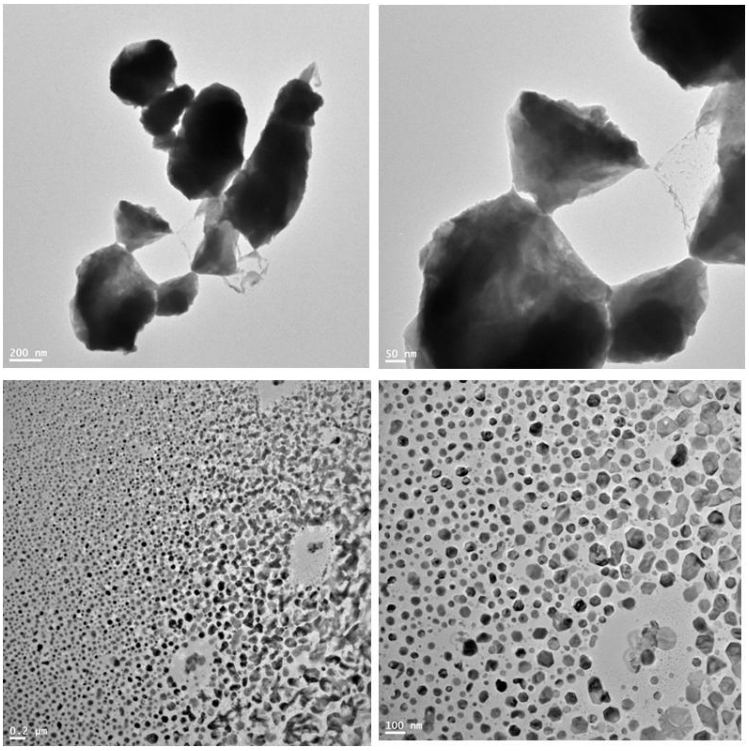

Fig. 3 Transmission electron micrographs (TEM) images of the ball-milled bismuth telluride powder.

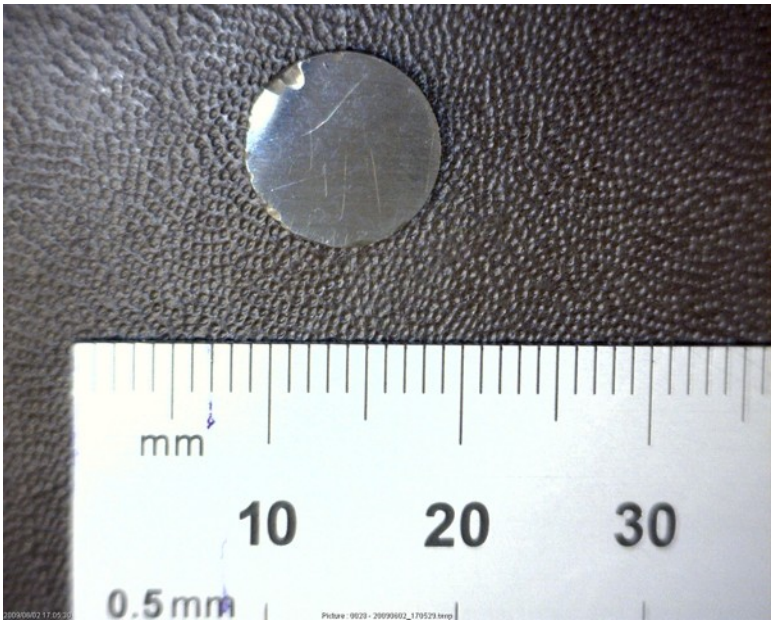

Fig. 4 Pellet of Bi_2Te_3 consolidated from ball-milled powder. The powder was pressed in a uniaxial press under a pressure of 50 MPa at 400°C for 1 hour.

c. Thermoelectric Transport in Wires (Champagne, Karki, Walker andYoung)

Our research has focused on the synthesis and characterization of novel intermetallic systems in reduced dimensions. By measuring the magnetotransport behavior of these materials in reduced dimensions, we gain insight into the physics driving the transport properties between the films and the bulk. We have just begun our initial investigation of the thermoelectric properties of films and fibers of MoN and Mo_3Sb_7, which have never been measured before. It's quite possible that the thermal conductivity in these advanced architectures can be reduced, thereby improving the materials overall thermoelectric performance.

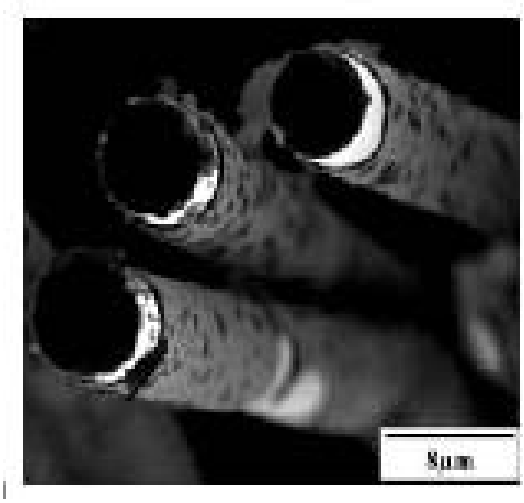

Figure 1. New microfibers of $ZnNNi_3$.

In addition, we have begun a study of the intermetallic $Ag_{8+\delta}GeTe_6$ (Ag816). This material in bulk form has one of the lowest thermal conductivities of any material, and as such, warrants further investigation as a potential thermoelectric. Furthermore, it is a mixed conductor, possessing both electronic and ionic contributions to its electrical conductivity. In our thermal transport study of this material, we discovered that the electrical resistivity is a function of the local Ag-ion concentration, which can be altered via application of an electric field (current). This moves the Ag ions from one end of the sample to the other via a network of vacancies in the crystal structure, thereby creating a resistivity gradient across the sample. This produces a large non-uniform Joule heating effect which is reversible with current direction (see Figure 2). Large temperature differences between the two ends of the sample can be maintained, since the thermal conductivity of the material is so poor. Simply by switching the direction of the current, we can change the direction of the temperature gradient. In some samples with a current of 100 mA, we are able to maintain a 100 ^{o}C temperature difference across a 1-cm long sample.

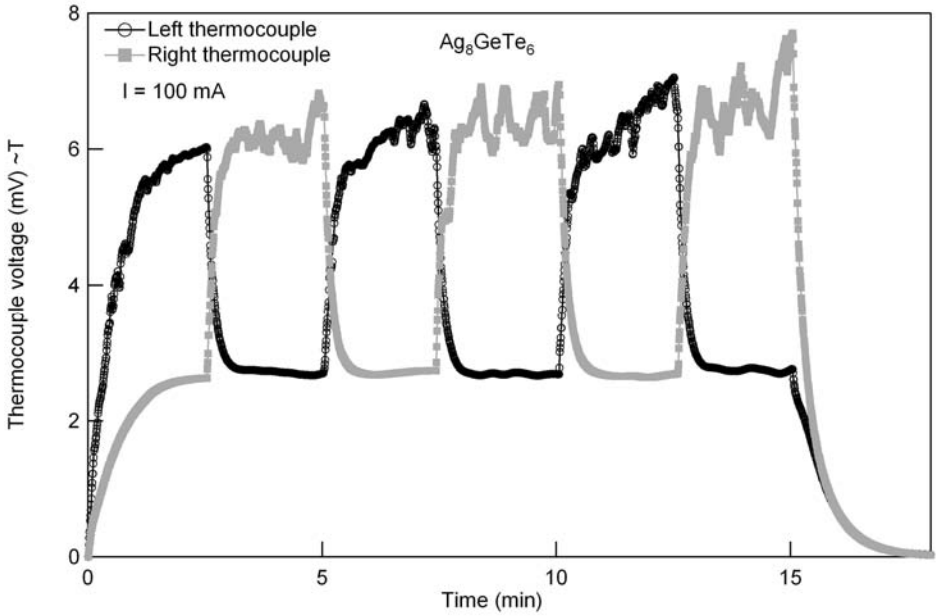

Figure 2. Plot of the thermocouple voltages attached to the two ends of a bar of Ag816. The left axis is proportional to temperature. Notice how the temperature gradient switches direction upon changing the direction of the current, for example, at 2.5 min and 5 min.

We have also made the Si version of the 218 material (Ag_8SiTe_6) as well as doped variants of the Ge compound, including: Se doping for Te and Cu doping for Ag. The hope is that through the chemical substitutions, we can reduce the electrical resistivity without adversely affecting the large Seebeck values and low thermal conductivity. There is a metal to semiconductor transition in the Mo_3Sb_7 system doped with Te. Good thermoelectrics tend to have carrier densities on the order of $10^{19}/cm^3$ By doping with Te, we can shift the Fermi surface toward a gap-edge in the density of states. We have begun the initial synthesis of this doped material. Our goal is to reduce the dimensions by synthesizing thin films via pulsed laser deposition (PLD).

This ongoing research program offers postdocs the opportunity to work on novel systems, provides graduate students with an avenue to perform dissertation directed research, and trains undergraduates in a variety of synthesis and characterization techniques. Overall, materials synthesis provides a natural bridge between teaching and research, especially for undergraduates. They are able to make real contributions in a relatively short amount of time. Nick Walker worked on this project last summer. He is an undergraduate biological science major from Nicholls State University and a participant in the Louisiana Biomedical Research Network (LBRN) Summer Research Program. Nick was an excellent student who made significant progress on the thermoelectric project in just several weeks. He presented his results during a poster session at the end of the program..
Considering the alternative energy aspects of thermoelectrics, and the new President's strong policy for increased funding in basic scientific research, new federal monies may emerge for thermoelectric research. We will pursue these opportunities in the upcoming year.

5. Work Products

d. Electrochemical storage materials (Gabrisch, Mohanty and Yi)

The main part of our research activities concerns the characterization of electrode material used in rechargeable Li-ion batteries by electron diffraction. During the past year we synthesized mixed transition metal oxides using a co-precipitation method and began a collaboration with Southern University for testing in Li-half cells. The combination of EELS and SQUID measurements proved a fruitful approach to better understand observed crystallographic transformations in Li_xCoO_2. The educational effort was realized by involving an undergraduate student in the research. A new undergraduate course : Introduction to Material Chemistry (CHEM 3610) has been developed by the PI and was taught for the first time in Fall 2008.

Experimental

$LiNi_{1/3}Mn_{1/3}Co_{1/3}O_2$ was prepared by the hydroxide co-precipitation method. Stoichiometric amounts of $NiSO_4 \cdot 6H_2O$, $CoSO_4 \cdot 7H_2O$ and $MnSO_4 \cdot H_2O$ with a Ni:Co:Mn ratio of 1:1:1 were dissolved in distilled water separately to produce concentrations of 2 $molL^{-1}$. Then the solutions were precipitated by adding aqueous NaOH solution and proper amounts of NH_4OH solution under Argon atmosphere. The solution was kept in Argon atmosphere for 24 h at 50 ^oC while maintaining a pH of ~10-11. The precipitate was filtered, washed with water and kept in a glove box overnight at 50 ^oC. The obtained precursor was mixed with 5 % excess $LiOH \cdot H_2O$ and thoroughly ground in a mortar. The powder was pressed into pellets and heated at 450^oC for 5h followed by heating at 650^oC for 9h. The disintegrated pellets were pressed again and calcinated at 850^oC for 18hrs to obtain $LiNi_{1/3}Mn_{1/3}Co_{1/3}O_2$. Chemical delithiation was performed under Argon atmosphere using NO_2BF_4 solution at a ratio TM : oxidant = 1 : 1.1 over 3 hours at room temperature. Subsequently portions of the delithiated powder were heat treated in air at 70ºC for 30 days. Commercial $LiNi_{1/3}Mn_{1/3}Co_{1/3}O_2$ and cycled cathodes prepared of the powder were obtained from ENAX Inc (generation 2, powder prepared according to the method published in [8]). The cathodes underwent 520 charge discharge cycles between 3.0 and 4.3V and were stopped in the discharged state.

Electron diffraction experiments were performed using the JEOL 2010 Transmission Electron Microscope at the University of New Orleans operated at 200 kV. Experimental diffraction patterns were compared to patterns simulated with the software Desktop Microscopist using unit cells published in literature, a list can be found in [1].

Results and Discussion

The in-house synthesized $LiNi_{1/3}Mn_{1/3}Co_{1/3}O_2$ showed no evidence of long range ordering, consistent with the low synthesis temperature of 850ºC. Out of 22 analyzed particles 20 were characterized by electron diffraction pattern typical for the O3 phase, which means that the TM ions are randomly distributed over the 3a lattice sites. A small fraction of particles (2 out of 22) showed spinel type reflections. Chemical extraction of Li from the synthesized particles did not introduce significant changes to the microstructure (estimated Li-content 0.75). This observation differs from observations in chemically delithiated Li_xCoO_2 where removal of small amounts of lithium results in the appearance of forbidden $\{1\bar{1}00\}$ reflections in the [0001] zone axis pattern. In $LiCoO_2$ O-Co-O slabs glide in the (0001) plane upon Li removal, which changes the stacking order and breaks the rhombohedral symmetry along the stacking direction of O-Co-O which gives rise to the observed $\{1\bar{1}00\}$ reflections. In $LiNi_{1/3}Mn_{1/3}Co_{1/3}O_2$ we observed very faint forbidden reflections, only in one out of 10 particles, see Fig. 1. This indicates an improved

structural stability of the mixed TM compound in comparison to $LiCoO_2$. Annealing of the delithiated particles increased the amount of spinel phase to approximately 40%. Additionally after annealing the morphology changes in some particles to a lamellar structure, see Fig. 2. A comparison of the analyzed particles is given in table 1.

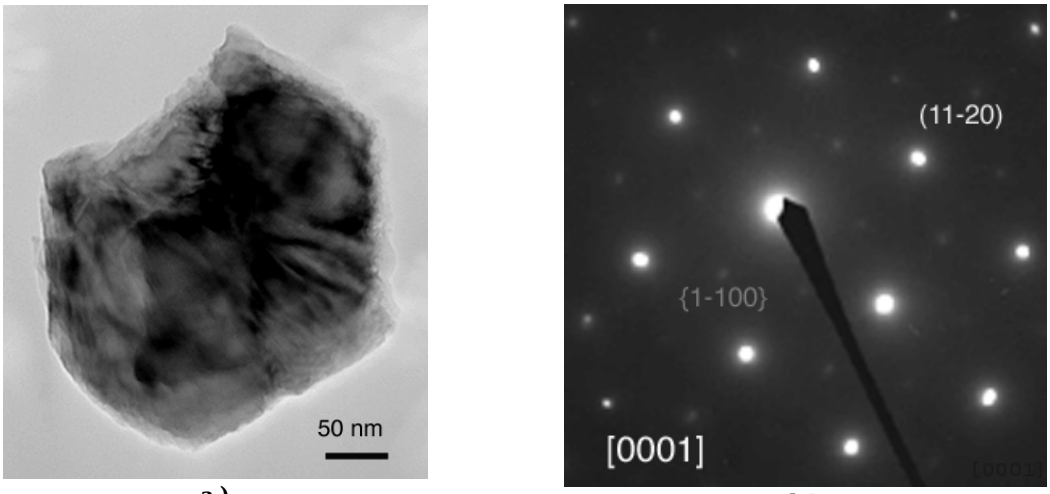

a.) **b.)**

Fig. 1 : $Li_xNi_{1/3}Mn_{1/3}Co_{1/3}O_2$ particle produced by chemical delithiation showing faint $\{1\bar{1}00\}$ reflections (see text).

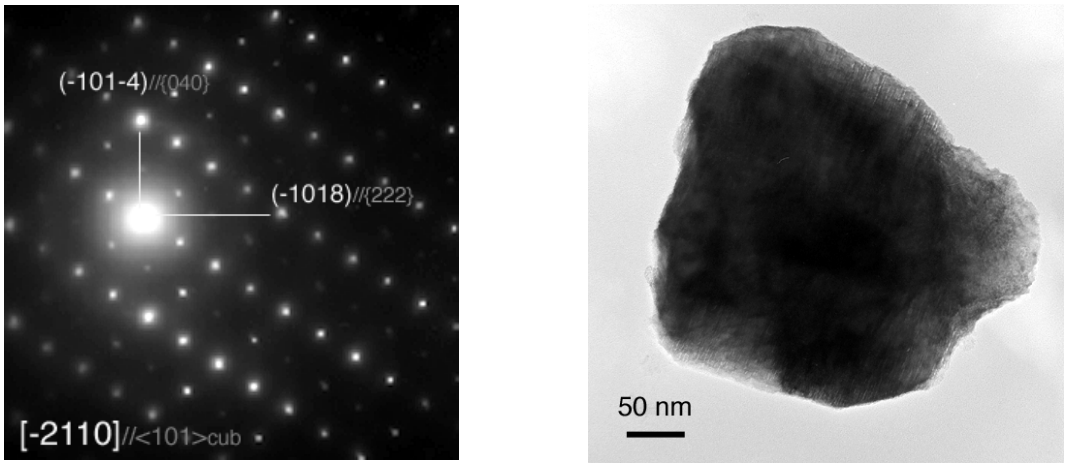

a.) **b.)**

Fig. 2 : $Li_xNi_{1/3}Mn_{1/3}Co_{1/3}O_2$ particle produced by chemical delithiation and annealing at 70ºC for 30 days. The diffraction pattern shows contributions of the O3 phase and fainter contributions of the cubic spinel phase, notice the morphology change near the particle surface.

Table 1 : Analysis of $LiNi_{1/3}Mn_{1/3}Co_{1/3}O_2$ synthesized at UNO (The numbers reflect the count of each category, all particles were single crystal, the total number particles analyzed is give in brackets at the top of each column.)

Classification	as synthesized (22)	delithiated (10)	delithiated, annealed (10)
O3	20	9	10
spinel	2	5	5
forbidden $\{1\,\bar{1}\,00\}$	0	1	0

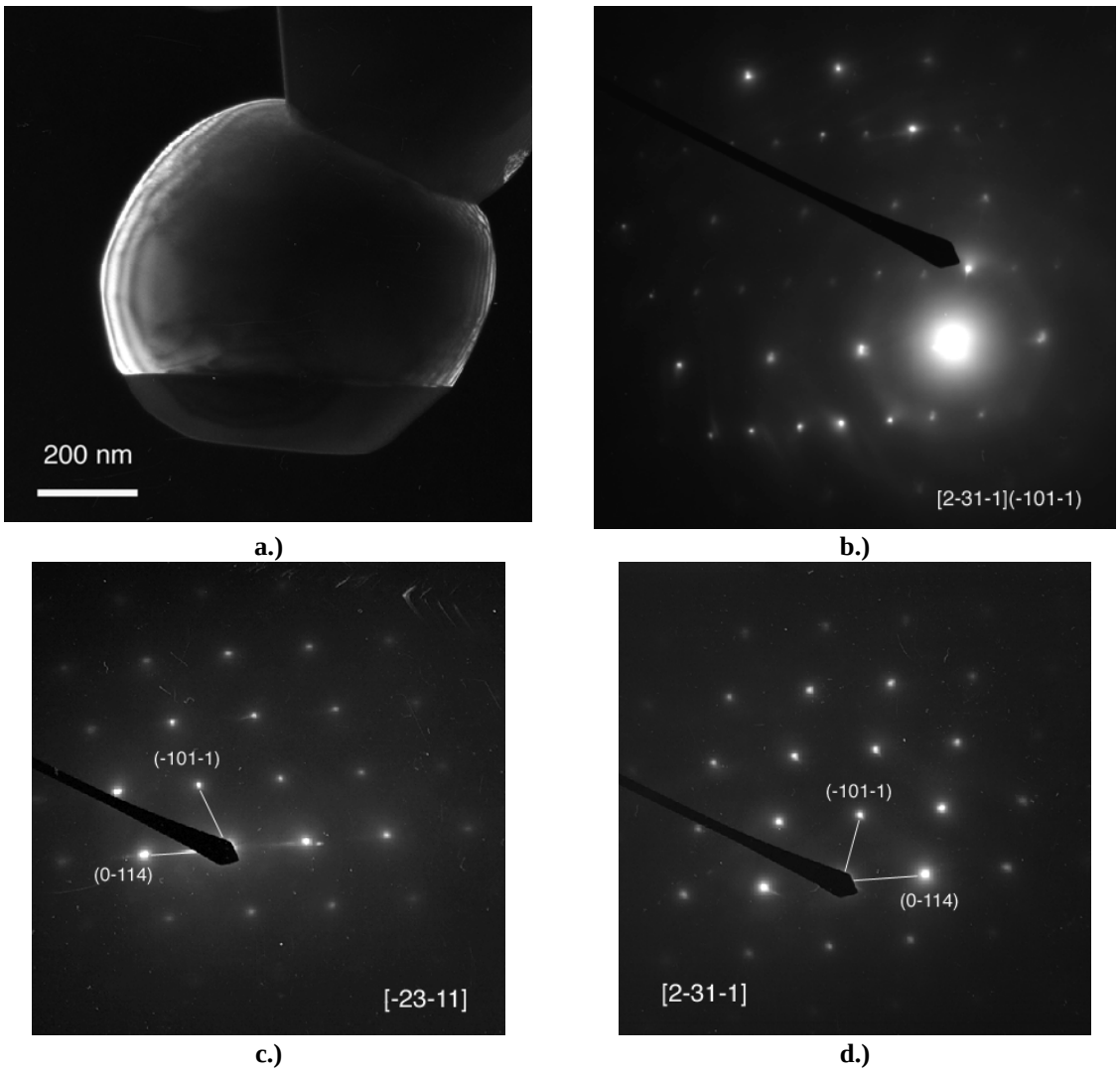

a.) **b.)** **c.)** **d.)**

Fig. 3 : Image and diffraction patterns taken from a pristine, commercial poly-crystalline particle. a.) dark field image taken with a reflection unique for the bright part in the image. b.) corresponding diffraction pattern, the reflection used for imaging is marked by the pointer. c. and d. show the diffraction patterns of the two crystals.

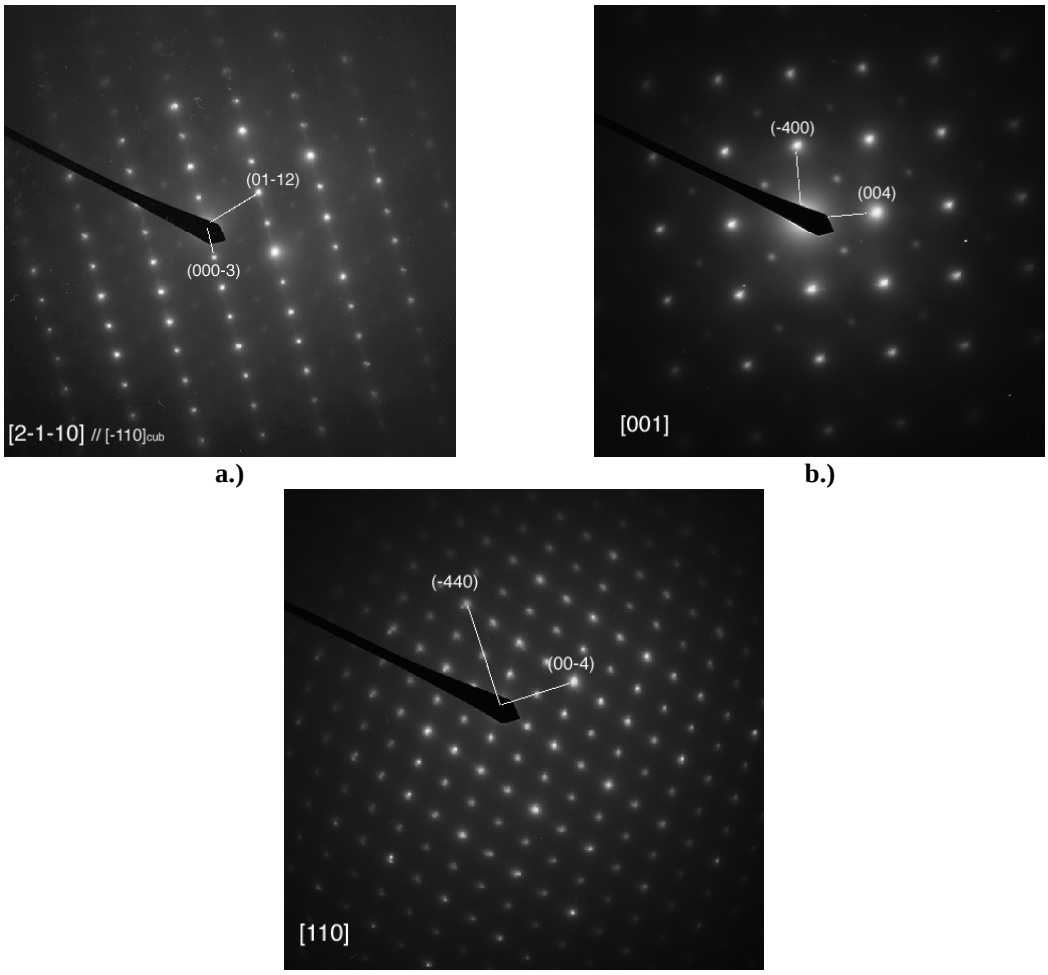

a.) **b.)**

c.)

Fig. 4 : Electron diffraction patterns showing spinel reflections of increasing intensity from a.) to c.) corresponding to a gradual cation rearrangement.

Table 2 : Analysis of commercial $LiNi_{1/3}Mn_{1/3}Co_{1/3}O_2$: the numbers reflect the count of diffraction patterns in each category. Some particles were poly crystals, the total number of analyzed patterns is given in brackets at the top of each column, 25 pristine particles, 15 cycled particles were analyzed.

classification	pristine (31)	cycled (17)
O3	22	6
spinel	5	8
$\sqrt{3}$ x $\sqrt{3}$ R30°	3	2
other	1	1

The commercially produced $LiNi_{1/3}Mn_{1/3}Co_{1/3}O_2$ obtained from ENAX Inc. revealed a less homogeneous picture than our synthesized material. The material is however more homogeneous than the generation-I material supplied by the same company[1]. We found that the pristine material has about 20% polycrystalline particles and a small amount of in plane long-range ordering corresponding to the $\sqrt{3}$ x $\sqrt{3}$ R30° unit cell. In most cases the polycrystalline

particles consisted of two crystals indexed as O3 phase that were related by a twin boundary (4 out of 5). An example is shown in Fig.3, where diffraction patterns of each crystal (Fig. 3c,d) are shown together with the superimposed pattern obtained from the whole particle (Fig. 3b) and a dark field image taken with a reflection unique to one crystal (Fig. 3a). The amount of poly-crystals was approximately constant in the particle population analyzed after cycling. Similarly the amount of long-range order remained constant before and after cycling, with 10% and 13% respectively. A change was however observed in the amount of spinel phase : during cycling the amount of spinel increased at the expense of O3 phase from 16% before cycling to 47% after cycling. In both samples the intensity of spinel reflections spans a wide range corresponding to a gradual change of the cation ordering between the two limiting phases : layered and cubic. This is illustrated in Figs. 4 a-c, where the typical spinel reflections are barely visible in Fig. 4a while they have an intensity identical to that of the fundamental reflections in Fig .4c. A summary of the analyzed particles of the commercial material is given table 2.

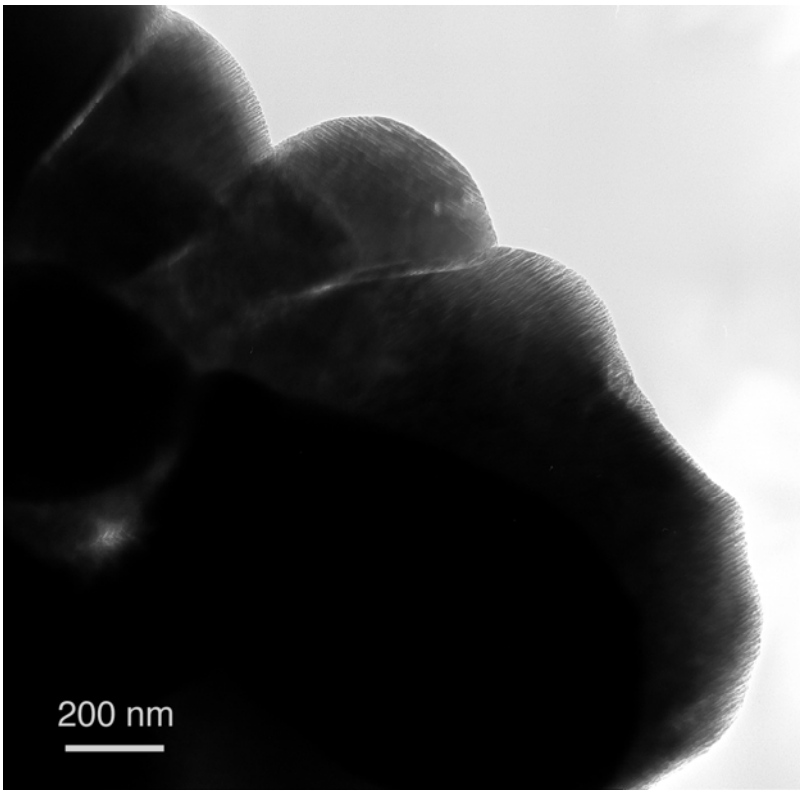

Fig. 5 : Transition Electron Microscope image showing an agglomerate of $LiNi_{1/3}Mn_{1/3}Co_{1/3}O_2$ particles with a mile feuille morphology observed after charge discharge cycling or ageing.

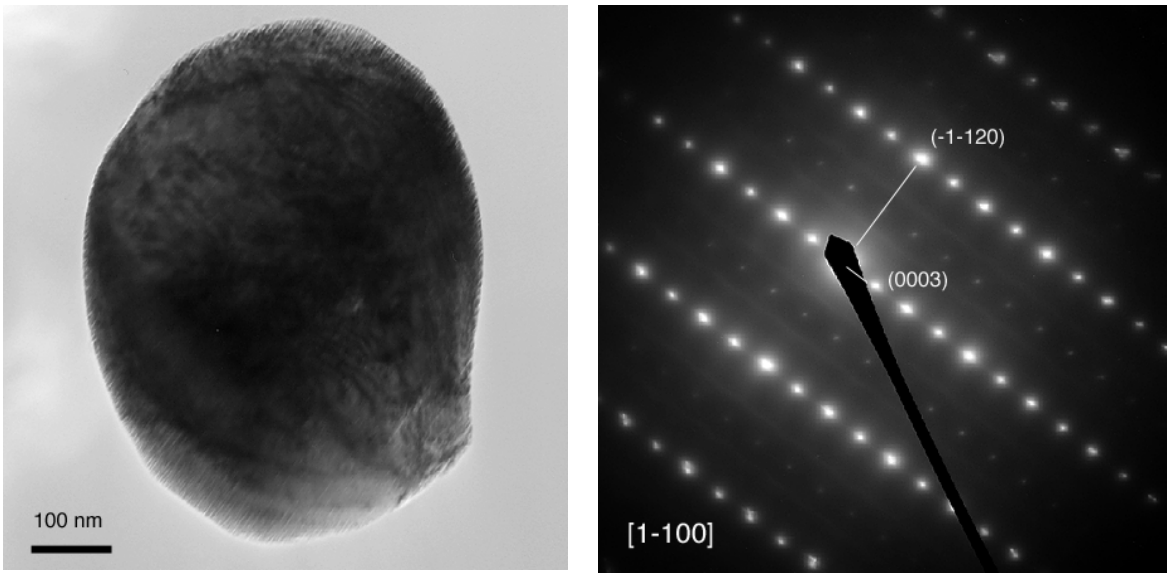

a.) **b.)**

Fig. 6 : Image and diffraction pattern illustrating the orientation relationship between the lamella in the mille feullie morphology and the diffraction pattern.

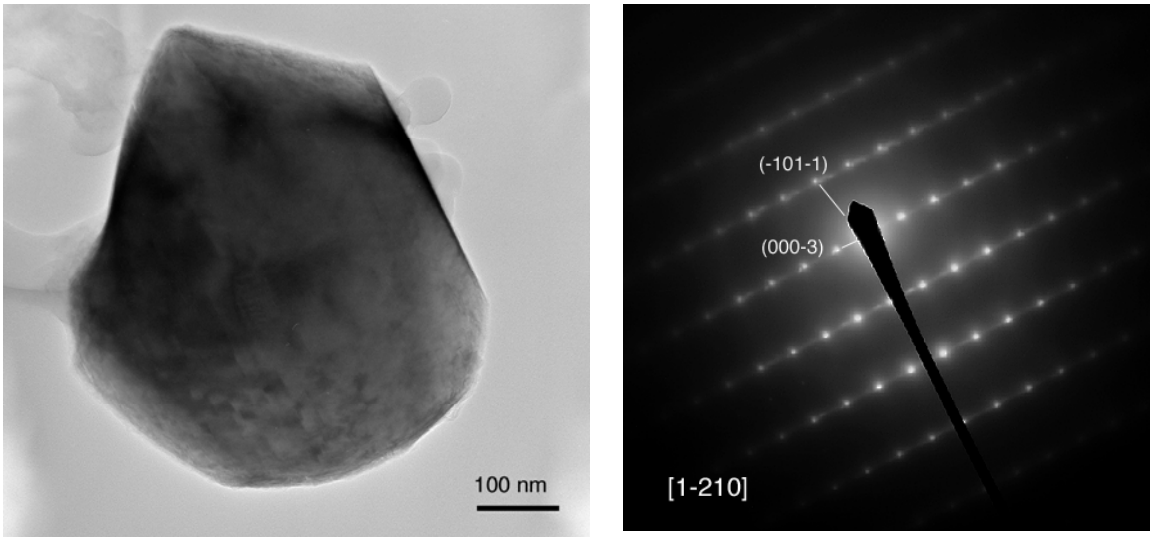

a.) **b.)**

Fig. 7 : Image and diffraction pattern of a cycled particle.

The most striking observation in the cycled particles is the change in morphology in some particles that is similar to that observed in chemically delithated particles after heat treatment, see Fig.5. Apparently the particles start to disintegrate during cycling or anneal and form a lamellar morphology that we name “mille feuille”. In Fig. 6 a mille feuille particle is shown together with its diffraction pattern. The diffraction pattern can be indexed as O3 phase, however faint contributions of spinel and $\sqrt{3}\,\mathrm{x}\,\sqrt{3}\,\mathrm{R30^o}$ ordering are also observed. A comparison between the directions in the diffraction pattern and in image illustrates that the

lamellas form between (0001) planes, where bonding between adjacent layers is weak. A loser look at the intensity of fundamental reflections in Fig. 6b shows that the shape is not circular but streaked along the [0001] direction. Streaking indicates the presence of either stacking faults or very thin platelets in planes perpendicular to the streaking direction, which are the (0001) planes. At this point it is not clear whether the observed mille feuille morphology is responsible for the observed streaking. In Fig. 7 a cycled particle is shown that does not have the mille feuille morphology, but has high amounts of streaking in the diffraction pattern. Altogether we observed streaking in 6 out of 15 particles analyzed after cycling, but only in one out of 22 of the pristine material.

Conclusions

$LiNi_{1/3}Mn_{1/3}Co_{1/3}O_2$ synthesized at 850ºC shows no in plane ordering and is structurally stable with respect to cation arrangement during chemical delithiation. After long-term anneal at 70ºC about 40% of the particles have a spinel structure and in some particles a the morphology has changed to a mille feuille type appearance. Commercial $LiNi_{1/3}Mn_{1/3}Co_{1/3}O_2$ synthesized at 1000ºC shows long-range ordering in about 10% of the analyzed diffraction patterns, a fraction that remains stable over charge discharge cycling. The pristine material consists to 70% of particles with random TM ions distribution on the 3a lattice sites, however after 520 charge discharge cycles a portion of these have transformed to spinel, so that about 47% spinel phase is observed after cycling. The mille feuille morphology is observed frequently after cycling. Streaking in the diffraction pattern of cycled particles indicates that microscopic defects have formed on (0001) planes.

Reference

[1] H. Gabrisch, T. Yi, and R. Yazami, Electrochemical and Solid-State Letter **11**(7) (2008) p. A119-A124.

e. Ferroic Materials (Malkinski)

This project deals with nonconventional methods of mutual conversion of electric to magnetic fields. One way of converting electric to magnetic field is developing multiferroic materials consisting of ferroelectric and ferromagnetic materials. More specifically, the ferroelectrics with superior electrostrictive properties can transfer over 90% of electric energy through elastic coupling to ferromagnetic materials with excellent magnetostrictive properties. The materials in the form of powders of ferroelectric PZT and PMN materials and ginat magnetostrictive Terfenol powder have been purchased to make composite materials. The first results showed that the elastic coupling between the grains of ferroelectric and ferromagnetic grains is essential for the performance of the composite. Two methods of binding have been explored: cold pressing and resin bonds. Both methods were found to have some disadvantages for the properties of composites. Cold pressing at smaller pressures cannot produce strong mechanical bonds between the hard grains. On the other hand, larger pressures change properties of the magnetostrictive material by inducing magnetic stress-anisotropy. These problems do not exist for resin bonding. However, in the case of indirect bonding the mechanical properties of the resin as well as the amount of the resin in between the grains are essential for the performance of the composite. It was found that too large amount of the resin absorbs the stresses and prevents efficient transfer of elastic energy between the grains of different kind. Another conclusion for the initial research

is that the elastic properties of the resin should match those of the ferroelectric and ferromagnetic grains as close as possible. The research will be continued to optimize these parameters. In addition hot pressing and sintering will be explored.

Recently Dr. Malkinski has been working on developing a new concept of a composite of organic molecules and inorganic nanoparticles which will display the properties of multiferroic materials. The general idea is to embed elongated magnetic particles into nematic liquid crystals. The elongate molecules of the liquid crystal while directed by an applied electric field will drag magnetic nanorods and change the direction of the magnetic field produce by them.

Both kinds of the materials may lead to applications in voltage controlled magnets, which will be lighter and more energy efficient compared to electromagnets, which require large currents and produce significant losses of energy due to heat dissipation.

f. Nanoassembly of nanoparticles and tubule nanocontainers (Lvov)

Halloysite clay nanotubes were investigated as a nanotubular container for the corrosion inhibitor benzotriazole. Halloysite is a naturally occurring cylindrical clay mineral with an internal diameter in the nanometer range and a length up to several microns, yielding a high aspect ratio hollow cylindrical structure. Halloysite may be used as an additive in paints to produce functional composite coating material. Maximum benzotriazole loading of 9 % by volume was achieved for clay nanotubes of 50 nm external diameter and lumen of 15 nm. Variable release rates of the corrosion inhibitor were possible in a range between 5 and 50 hours as was demonstrated by formation of stoppers at tube openings. The anticorrosive performance of the sol-gel coating and paint loaded with 2-5 % of halloysite entrapped benzotriazole was tested on copper and on 2024-aluminum alloy by direct exposure of the metal plates to corrosive media. Kinetics of the corrosion spot formation at coating defects was analyzed by the scanning vibrating electrode technique with essential damping of corrosion development demonstrated.

Halloysite / paint nanocomposite coating In Fig. 1, SEM micrograph of halloysite nanotubes in scratched paint layer is shown. Nanotubes are exposed to external environment at paint scratch or cracks. Benzotriazole loaded halloysite will start enhanced release of the inhibitor when a crack the occurred, protecting the metal underneath from corrosion development.

Fig. 1. SEM micrograph of paint scratch containing 5 wt % of halloysite nanotubes in it

Halloysite is readily mixed with a variety of metal protective coatings which is an important advantage for this material. Water contact angle for halloysite pressed in the tablet was found as low as 10 ± 3º but it still was easily wet with paint, probably due to its highly porous surface. Surprisingly, for paint droplet the contact angle was even less, of ca 3 º. Paint droplets spontaneously spread over the halloysite tablet, which is an indication of good wettability of the halloysite surface by paint. The reason for this could be due to specific chemical interactions (like Van Der Waals interaction) between surface OH groups and paint CH groups.

Addition of nanotubes into industrial oil based paint significantly improved the strain – stress characteristics of the metallic coating as it is demonstrated in Fig 2. Threefold increase of paint tensile strength was observed with addition of 5 wt % of halloysite (0.7 MPa for pure paint versus 1.9 MPa for 5 wt % halloysite loaded paint). Halloysite fillers also increases the hardness of the paint. An elastic modulus of the dry paint samples was 16.3 MPa for the layer of pure paint and 23.1, 34.6, 69.3 MPa for 2 wt %, 5 wt %, and 10 wt % composite of halloysite with paint, respectively. However, paint films became brittle with loadings greater than 5 wt % halloysite. These data correspond to results on halloysite clay / polymer bulk composites. For example, incorporation of 5-13 % of halloysite in polypropylene resulted in 30-50 % strength increase. Therefore, from the point of view of paint cover strength, an optimal loading is approximately 5 wt %.

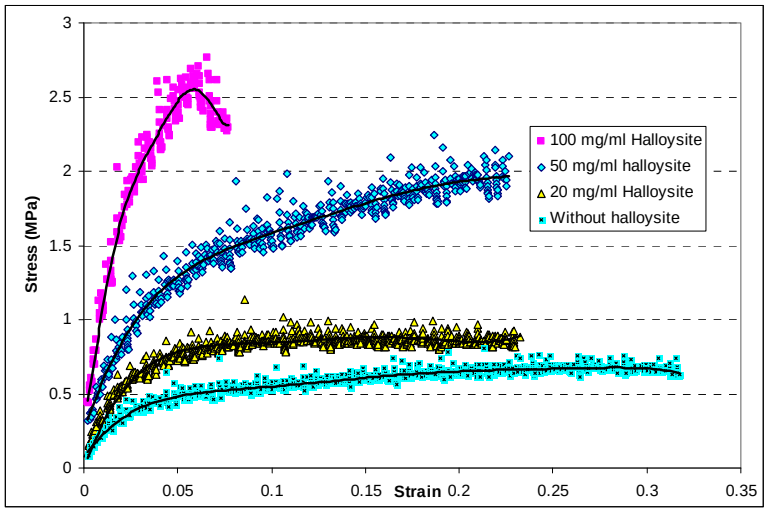

Fig.2. Stress strain relationship of industrial oil based blue paint. Concentration of halloysite is shown in milligrams of added halloysite per milliliters of wet paint.

Enhanced corrosion protection with benzotriazole loaded hallosyite The initial stages of corrosion development in metal coatings and self-healing ability of the halloysite-doped film were analyzed with scanning vibrating electrode technique on 2024-Al alloy (taken as a substrate), which contains 4 wt % copper. Alloy plates were coated by dip-co ating procedure with ZrOx-SiOx sol-gel layer and artificially scratched. Both samples with and without inhibitor-loaded halloysites were immersed in corrosion solution and corrosion development was observed over 24 hours as maps of the corrosion current. Anodic corrosion activity on the aluminum alloy coated by simple sol-gel layer was high and rapidly increased within several hours in the scratched area. This indicates a fast pitting corrosion process taking place at the artificially introduced defect(s). In case

of alumina coated with sol-gel containing halloysite tubes filled with benzotriazole, the rate of corrosion at the defect points is strongly reduced in the first moment of corrosion and almost no corrosion current (both cathodic and anodic) was observed. Compared to the pure sol-gel coating, maximal current density in this case was 6 times smaller (ca. 3 μA/cm² for inhibitor containing sol-gel and 18 μA/cm² for pure sol-gel after 24 hours of immersion), which points out very strong anticorrosion self-healing effect caused by controlled release of the inhibitor from the halloysite nanotubes in the cracked area.

Summary: Halloysite nanotubes are a promising material for entrapment of corrosion inhibitors into paint due to its viability and compatibility with variety of water or oil based coatings. Benzotriazole was loaded in 50 nm diameter halloysite tubes and admixed to paint coating in the amount 2-5 wt %. A tensile strength of such nanocomposite paint coating increased approximately in 2 times. Benzotriazole release from raw halloysite nanotubes extended for ca 5 hours, and its kinetics was fit with power function model. Corrosion inhibition efficiency of halloysite nanocontainers for aluminum and copper samples was demonstrated by monitoring the localized corrosion current density on scratched as well visually by exposure of scratched metal sample to highly corrosive environment showing significant reduction in metal corrosion rate.

C. Opportunities for Faculty Recruitment, Retention and Development Post-doc, Graduate and Undergraduate Student Training

- Seven graduate students and four undergraduate students are currently involved in training under this project, (five from La Tech/IfM, three from UNO and three from LSU).
- Undergraduates who were trained in the project: Michelle Sibille, Enkhjin Bayarsaikhan, and Chris Chain. Michelle Sibille has been accepted to medical school for fall 2009. Master's level graduate students: Raj Masvekar, Jessica Wasserman, and Dustin Green. Raj Masvekar and Dustin Green have been accepted into Ph.D. programs away from Tech for fall 2009 and Jessica Wasserman has been accepted into the Ph.D. program in Biomedical Engineering at Tech for Fall 2009. Post doc Dr. Mangilal Agarwal worked for the project for one year.

D. Partnership Activities

- Stokes (UNO) has partnered with Nanohmics, Inc. (Austin, TX) and United Technologies Research Center on a project concerning flexible thermoelectric devices.
- Drs. Lvov and Decoster –AMRI annual conference in February 2009, and discussed results with AMRI researchers. Two joint reports were presented at AMRI Mardi Gras symposium. With Prof. Kevin Stokes, we are working on preparation of the project on clay nanotube smart nanocontainer for anticorrosion coating.

E. Problems Encountered

- Second year funding for LaTech/IfM was delayed for six months and money received in December 2008, therefore, again we will need extension till December 31, 2009.

3. **Contributions:**

- Constructed a sample holder that will allow us to measure the Seebeck coefficient of thin films. The holder is designed to fit on a transport puck from the Quantum Design PPMS system, so that the temperature dependent thermopower can be measured.
- Constructed a "ZT-meter", which utilizes Harman's method to directly measure the thermoelectric figure of merit of a material. Currently, the meter can be used at room temperature. Having this device available will greatly facilitate in the screening of many new materials for improvement in their thermoelectric properties.
- "Clay Nanotubes for Controlled Release of Corrosion Inhibitors," NASA-EPSCOR LA BoR, pre-proposal, PI, $200,000, Jan 2010-Dec 2011.
- "Clay Tubule Nanocontainer for Responsive Corrosion Protection," NSF-nanomanufacturing, PI, $270,000, Sept- 09- Aug 20012
- 'Microfluidic Device for Directed Assembly of Nanoparticles and Polyelectrolytes on in situ Generated Templates," NSF-Nanomanufacturing, PI, $280,000, Sept- 09- Aug 20012
- "Materials Synthesis in Clay Nanotubes," PI, NSF, $340,000, Sept 2009- Aug 2012
- "Clay Tubule Nanocontainer for Responsive Corrosion Protection," NSF-nanomanufacturing, PI, $270,000, Sept 09- Aug 2012
- 'Collaborative Research: Microfluidic Device for Directed Assembly of Nanoparticles and Polyelectrolytes on in situ Generated Templates," NSF-nanomanufacturing (with Virginia Tech), PI, $280,000, Sept- 09- Aug 20012

4. **Project Revision**

- Dr. Despina Davis replaced as co-PI Kody Varahramyan with responsibility for the thermoelectrics project at IfM.

5. **Work Products:**

Papers:

A.B. Karki, D.P. Young, P.W. Adams, E.K. Okudzeto, and J.Y. Chan, "Critical current behavior of superconducting MoN and Mo3Sb7 microfibers", *Phys. Rev. B* **77**, 212503 (2008).

A.B. Karki, Y. M. Xiong, D.P. Young, and P.W. Adams, "Superconducting and magnetotransport properties of ZnNNi3 microfibers and films", submitted.

J. Zhang, A. Kumbhar, J. He, N. Das, K. Yang, J.-Q. Wang, H. Wang, K.L. Stokes and J. Fang, "Simple Cubic Super Crystals Containing PbTe Nanocubes and Their Core-Shell Building Blocks," *J. Am. Chem. Soc.* **130**: 15203-15209 (2008).

N. Veerabadran, Y. Lvov, R. Price, "Organized Shells on Clay Nanotubes for Controlled Release of Macromolecules" *Macromolecular Rapid Commun.,* v.24, 99-103, 2009. featured on the journal cover page.

T. Shutava, S. Balkundi, Y. Lvov, "Epigallocatechin gallate/gelatin layer-by-layer assembled films and nanocapsules," *J. Colloid Interface Science,* v.330, 276-283, 2009

R. Mannam,M. Agarwal, A. Roy, V. Singh, K. Varahramyan, D. Davis, "Electrodeposition and Thermoelectric Characterization of Bismuth Telluride Nanowires," *J. Electrochemical Society* **156**, 8, 2009

Presentations:

1. "Nanostructured Thermoelectric Materials," K.L. Stokes, Dept. of Chemistry and Physics Seminar, Southeastern Louisiana University, Apr. 3, 2009. (invited)
2. Q. Xing, S.Chen, M. DeCoster Y. Lvov, "Porous 3D Cellulose Fiber Based Microscaffold for Cell Culture," TERMIS-NA 2008 (Annual Conference of Tissue Engineering & Regenerative Medicine International Society), San Diego, Dec 10, 2008.
3. S. Madisetti, Z. Zheng, Y. Lvov, L. Que, "Layer-by-Layer Nanoscale Coating of Microparticles with Droplet Microfluidic Device," 4th Annual International Conference on Nano, Micro Engineering and Molecular Systems, IEEE-NEMS'09, Shenzhen, China, Jan 8-12, 2009
4. D Fix, Y. Lvov, H. Möhwald, "Inhibitor Loaded Halloysite Nanotubes for Corrosion Protection," International Conference NanoMaterials-2009, Lisboa, Portuguese, April 5-8, 2009.

PKSFI Report for LEQSF(2007-12)-ENH-PKSFI-PRS-04

Matthew A. Tarr
(PKSFI Broader Impacts, 2008-2009)

Broader Impacts (Educational and Commercial Outreach)

1. **Personnel:** List all key personnel and other staff who provided *significant* contributions to the project. Provide information about the types of contributions made by each listed participant and controls in place to ensure that these contributions are adequate to the project's requirements.

Matthew Tarr, Professor, Dept. of Chemistry, University of New Orleans – planned and coordinated academic year outreach activities (ScienceReach program) with subcontractor, Communities In Schools of New Orleans (CISNO); reviewed CISNO quarterly reports; presented program updates at quarterly meetings; conducted site visit to CISNO to evaluate subcontractor progress; coordinated planning and recruiting for summer outreach program (10 high school student participants for the summer 2008 program and 12 participants for the summer 2009 program). Supervised by project PI, Dr. Charles O'Connor.

Sara Massey , Director, Communities In Schools of New Orleans – directed all activities carried out by CISNO including academic year outreach programs in two New Orleans public or charter schools. Responsible for hiring and supervising ScienceReach program coordinator. Evaluated via quarterly reports submitted to Dr. Tarr and by site visits conducted by Dr. Tarr.

Brittany Morgan, ScienceReach Coordinator, Communities In Schools of New Orleans – implemented academic year outreach activities. Directly supervised and evaluated by Sara Massey.

2. **Activities and Findings:**
   - Describe major research and educational activities undertaken in this reporting period

The major focus of this project during the first project year has been on developing an academic year outreach program that targets New Orleans public or charter schools.

During this project year, the ScienceREACH program worked in four schools; McMain Secondary School, Sarah T. Reed High School, Martin Luther King, Jr. Charter for Science and Technology, Fischer Elementary. The programs implemented included; Rocketry Program, Forensics After School Program, Engineering Activities, Presentations, College STEM Major Lunches, Field Trips, In-Class Assistance, a College Day, a Science Fair, College Assistance and Tutoring/Mentoring, which combined reached a total of 204 students across 225 sessions.

(1) Rocketry Program: The Rocketry was an afterschool program at McMain Secondary School. Students built rockets under the supervision and guidance of David Koscielniak as part of the Team America Rocketry Challenge (TARC). The program served a total of 40 students across 26 sessions.

(2) Forensics After School Program: The Forensics Program was another component of the afterschool program at McMain Secondary School. In the Forensics Program students were exposed to the many STEM fields working within forensics including; Computer Forensics, DNA Analysis, Chemical Forensics, Forensic Anthropology, Forensic Pathology, and handwriting analysis. The forensics program engaged various professional from New Orleans Universities; Forensic Anthropologist John Verano from Tulane University, Dr. Golden Richard and Dr. Jaime Nino from the Computer Sciences Department at the University of New Orleans, and Dr. Paula Gregory and Dr. Dana Troxclair from the LSU Health Sciences Center all worked with the program to maximize the experience for the ScienceREACH students. The Forensics Program served a total of 40 students across 14 sessions.

(3) Engineering Activities: Engineering Activities were a third component to the after school program at McMain. There were 2 sessions devoted to exposing students to the basic principles of engineering and careers in the field. In one session students worked to build structures from simple materials such as spaghetti and marshmallows, and in the other students heard a presentation on civil engineering and bridge construction from Patrick Ibert, a civil engineer. This is Patrick Ibert's second year working with ScienceREACH. He also gave presentations to ScienceREACH students in the 2007-08 school year. A total of 22 students were served.

(4) Presentations: For the 2008-09 Program Year there were 13 college student and professional scientist presentations. Students in general chemistry at Tulane University gave 6 presentations on different areas within chemistry, including two presentations on atmospheric gases, two presentations on polymers, and two presentations on endothermic and exothermic reactions to 35 students at McMain. There were also three presentations at McMain given by graduate students at Tulane University; one student gave a presentation on Evolutionary Biology to 34 students, one student gave a presentation on Ornithology to 15 students, and another student in Evolutionary Biology and Ecology gave a presentation to 20 students on his research on insects in Costa Rica. There were also two presentations at McMain given by UNO Students in the STARS Program who talked to the science club and Mr. Lewis's Computer Science Class about different areas of computer science. Jost Goettert also gave a presentation to 30 students at Sarah T. Reed High School. His presentation focused on nanotechnology, and was given to chemistry classes.

(5) College STEM Major Lunches: There were 5 College STEM Lunches at McMain, which exposed 91 students to college students in the STEM Fields. The lunches served as an opportunity to connect high school and college students, and provided high school

students with the opportunity to ask candid questions about college life. The College STEM Major Lunches engaged college students from UNO, who talked about Computer Sciences, Xavier University students, who talked with about Pharmacy, Chemistry, Accounting, and Marketing, and Tulane University Students who talked about Evolutionary Biology and Ecology.

(6) Field Trips: Students involved in ScienceREACH went on a total of 7 field trips. Students from Sarah T. Reed High School took a field trip to the NASA Facilities at Michoud. Students at McMain attended 6 field trips to; UNO Computer Sciences Labs, WWL-News 4 Weather Center, NASA Facilities at Michoud, NASA Facilities in Stennis, Mississippi, an Allied Health Fair at Delgado Community College, and the Tulane University Neuroscience Labs. All field trips incorporated elements of the program, such as the rocketry program and NASA, or were a result of student interest and intended to further expose students to opportunities in the STEM fields.

(7) In-Class Assistance: Kathleen Darce, a UNO Education and Chemistry Major, worked in Mrs. Ryes Chemistry class at McMain Secondary to teach lessons, perform experiments, and assist Mrs. Ryes with other elements that contributed to an improvement in the class experience and quality. Kathleen worked with 17 students in Mrs. Ryes class for 1-2 hours per session for a total of 8 sessions.

(8) College Day: On January 17, 2009 ScienceREACH and Communities In Schools hosted a College Day in association with the Martin Luther King Jr. Day of Service at Loyola University. The ScienceREACH Coordinator planned the program, which included 34 high school students and over 30 volunteers from UNO, Dillard University, Xavier University, Tulane University, and Loyola University. The day was an opportunity for high school students to meet in small groups with college students and ask candid questions about college life, as well as review the Common Application and the college admissions process, and listen to college student's experiences. The high school students also received tours of Tulane University and Loyola University, as well as attended a panel with admissions counselors from UNO, Tulane, Dillard, and Loyola.

(9) Science Fair: ScienceREACH assisted Reed High School with its science fair, providing materials and assistance to students as they planned their projects, and then the ScienceREACH Coordinator, along with Jon Larson, the Americorps member assisting with the ScienceREACH Program, judged the projects.

(10) College Assistance: The ScienceREACH Coordinator has also helped students enrolled in the program with the college admissions, search, and ACT Registration process. The coordinator worked with 2 students to help them register for the ACT, as well as worked

individually with students to help them pick colleges that had the science majors they were interested in, and helped them map out their college classes and requirements.

(11) Tutoring/ Mentoring: Jon Larson, the ScienceREACH AmeriCorps member has tutored students in science and math at Reed, McMain, MLK and Fischer Elementary. In total he has tutored students for 212 hours.

a. Reed - 44 students for a total of 90 hours on 22 days
b. MLK - 1 students for a total of 22 hours on 22 days,
c. McMain - 3 students for a total of 12 hours on 12 days
d. Fischer - 5 students for a total of 88 hours on 33 days.

In addition to individual tutoring and mentoring, Jon has also worked in Mr. Judson's AP Physics Class, helping students on their labs. CIS provided AP Physics study guides to Reed High School with funding from a California funding group, for the students in the class had no textbooks and the teacher had only the preparation test teacher guide from which to work.

Number and type of interactions with UNO personnel: 48

There have been 15 interactions with UNO Personnel. The ScienceREACH Coordinator continues to cultivate the relationship with the UNO STARS Program. Dr. Jaime Nino was connected with a student at McMain Secondary School who has been accepted to UNO and intends to major in computer sciences. The coordinator has also worked with 8 students involved in the STARS program; Blandon Helgason, Andrew Case, Danielle Showmake, Therese Landry, Rupal Shah, Nathan Simpson, Jeremy Lay, and Andrew Cristina. Kathleen Darce has also worked with ScienceREACH at McMain, helping with science club and provided in-class assistance to Mrs. Ryes Chemistry Class. The coordinator also worked with Andy Benoit from the Admissions Office in order to plan for a UNO Admissions counselor to be present at the college day, and with Lynn Dupont from the Geography Department for GIS consultation. The ScienceREACH Coordinator also gave a presentation at the AMRI Mardi Gras Symposium on the Outreach Efforts of UNO and AMRI through the program.

ScienceREACH also continues to work with Lynette Bates of UNO's Upward Bound Program to provide the STEM enrichment portion of the Upward Bound Summer Program. In addition, we have worked with Juana Ibanez who works in the Geography Department. Juana has helped connect ScienceREACH to Marko Allain, who will be volunteering with Communities In Schools and ScienceREACH in our GIS Summer Program.

- Describe and provide data supporting the major findings resulting from these activities

This project reached a total of 204 students across 225 different sessions. Details of the number of students in each sub-program are presented in the section above.

Results: Student Reflections and a sample of the ScienceREACH Survey can be found at the end of the report.

For the 2008-2009 School Year the ScienceREACH Coordinator created a survey for students in order to track the effectiveness of the program. The results of the survey were as follows;

-100% of students know at least 10 Careers or more in the sciences as a result of the program
-100% of students said that they have learned more about STEM Professions and what type of education is required to reach them since being involved in the Program
-90% of students have reported that the program has increased their interest in Science
-Each student involved in the program has gained interest in at least 2 new areas of science, with most students now interested in careers in Engineering/Physics, Chemistry, and Computer Sciences
-100% of students want to go to college
-90% of students believe that the college lunches and talks with college students have helped to answer their questions about college
-Students also wrote reflections on the program, which supported this information. Students commented on how they were exposed to many different science careers, were supported in further exploring the careers that they were already interested in, and either increased or maintained their desire to pursue STEM Fields in college.

Efforts to expand funding and partnerships

CIS wrote two funding proposals which were not funded this year; however both funders have been cultivated and have encouraged submission of another application next year. The first was the Coypu Foundation to whom CIS wrote a proposal for $50,000 to fund the development and implementation of the Science of Natural Disasters program. Coypu did not fund any education-oriented projects in that round. The second was to the Environmental Protection Agency to expand upon the popular Sunship Earth program provided by Teaching Responsible Earth Education that would have guided 7th graders through a careers component. CIS continues to seek funding opportunities to expand its experiential offerings to students, as we continue to believe that exposure to careers in the STEM fields is one of the best ways we can bring relevance of academic work in the classroom to the attention of students.
Under development are two additional components: exposure to GIS mapping skills and the science of sports. These initiatives will take additional funding to develop.

- Describe the opportunities for faculty recruitment, retention and development, as well as post-doc, graduate and undergraduate student training provided by your project

There have been 15 interactions with UNO Personnel. The ScienceREACH Coordinator continues to cultivate the relationship with the UNO STARS Program. Dr. Jaime Nino was connected with a student at McMain Secondary School who has been accepted to UNO and intends to major in computer sciences. The coordinator has also worked with 8 students involved in the STARS program; Blandon Helgason, Andrew Case, Danielle Showmake, Therese Landry, Rupal Shah, Nathan Simpson, Jeremy Lay, and Andrew Cristina. Kathleen Darce has also worked with ScienceREACH at McMain, helping with science club and provided in-class assistance to Mrs. Ryes Chemistry Class. The coordinator also worked with Andy Benoit from the Admissions Office in order to plan for a UNO Admissions counselor to be present at the college day, and with Lynn Dupont from the Geography Department for GIS consultation. The ScienceREACH Coordinator also gave a presentation at the AMRI Mardi Gras Symposium on the Outreach Efforts of UNO and AMRI through the program.

ScienceREACH also continues to work with Lynette Bates of UNO's Upward Bound Program to provide the STEM enrichment portion of the Upward Bound Summer Program. In addition, we have worked with Juana Ibanez who works in the Geography Department. Juana has helped connect ScienceREACH to Marko Allain, who will be volunteering with Communities In Schools and ScienceREACH in our GIS Summer Program.

- Describe the nature and scope of partnership activities

  CISNO served as the primary agency for design, coordination, and implementation of all academic year outreach activities as described above.

- Describe any problems encountered during the last year of project activities.

  No problems were encountered.

3. **Contributions:** Summarize efforts made to build research and education capacity, secure external federal and private-sector funding, build infrastructure, contribute to economic development, and ensure project sustainability over the long term.

Academic year outreach programs were designed to attract high school students into college study in science and engineering fields. All schools targeted in this study have student bodies that are majority African-American. Furthermore, these schools have a high percentage of students receiving reduced or free lunch. Developing these human resources will provide a stronger base for science and technology development within the state of Louisiana.

A preproposal was submitted to the National Science Foundation's IGERT (Integrative Graduate Education and Research Traineeship Program) program. This program provides funding for training of graduate students in science and technology fields. If funded, this project will provide a unique training experience to graduate students which will develop within them a broad understanding of how science and technology fits into economic, social, and international issues. The proposal is pending as of submission of this report (June 2009).

4. **Project Revision:** Provide a listing of and explanation for any significant changes in the work plan for upcoming year, including any changes in the amount of investigators' time devoted to the project. If you made significant changes to the project design as outline in the proposal during the past year, please list and explain the changes, the purposes for the changes, and the results.

Several programs developed by CISNO will continue to be implemented in project year three. Refining of these programs will be undertaken in order to make them more efficient, but no major changes are foreseen. Efforts will be made to increase the number of undergraduate students involved in the project.

5. **Work Products:** List any tangible products (e.g., research publications and/or presentations, patents, licensing agreements etc.). Please combine all products into one document.

"Effects of atrazine on embryonic development and hatching of Japanese medaka (Oryzias latipes)," Theriot, J.; John, T.; Tarr, M. A.; Rees, B. B. 237th ACS National Meeting, Salt Lake City, UT, March 22-26, 2009.

PKSFI Report for LEQSF(2007-12)-ENH-PKSFI-PRS-04
Leszek M. Malkinski
(PKSFI-ESIP Clean Room, 2008-2009)

Title: Nanodevice Processing Laboratory

1. Personnel:
Leszek Malkinski, Associate Professor of Physics and Materials Science. Dr. Malkinski is in charge of design and management of this part of the project.

2. Activities:

The aim of this project is to provide research support for AMRI and collaborating institutions with the cleanroom facilities and technology to do competitive research in the field of nanofabrication. The evaluation of the purity of the air is based on number of dust particles in a unit volume. "Class 1000" cleanroom is the minimum requirement for the research activities on nanotechnology. This requirement was exceeded by designing a higher class purity cleanroom with re-circulating air. Due to this design the air is filtered several times before leaving the cleanroom and the number of particles present in the unit volume dropped to below 100, which elevates the rank of the cleanroom to "class 100".

In the period from July 2008 to June 2009 the following activities have been performed in relation to the Nanodevice Laboratory:
- UNO Services prepared room SC2041 for the installation by removing old floor tiles and leveling the floor, preparing the electrical and plumbing installations and repairing the roof.
- CEI Manufacturing Inc., selected through a bid process, started installation in the middle of July and major construction works have been completed by the end of September.
- Initial testing by independent company ENV Services, showed that the Nanodevice Processing Laboratory meets requirements of cleanroom "class 100" in terms of air purity. However, the pressures in the laboratory and the ante-room slightly exceeded acceptable standards.
- Corrections have been made in the airflow circulation to adjust the pressures to the acceptable levels. This work was completed in December 2008
- Following these modifications the laboratory was re-tested and on December 12, 2009 and a Certificate of Compliance was issued by the ENV Services stating the laboratory meets ISO Class 5 standards, which translates into "class 100". At this moment the payments were made for the CEI for the installation.
- Particle monitoring system has been purchased and installed for continuous monitoring of the air purity in the laboratory. During the certification process the readings of our particle monitoring system were compared and found consistent with the readings of the instruments used by the ENV Services.
- In January of 2009 we began moving and installing and testing the equipment in the Laboratory. In particular the mask aligner and UV exposure station as well as spin-coater/ hot plate were assembled and tested. Installation of the ion milling system was completed by the technician form the AJA International Co. in April 2009. At this moment the Nanodevice Processing Laboratory was open for the qualified users.

- At the beginning of June 2009 a series of training sessions for the users began. The sessions will prepare several students and postdoctoral researchers how to follow cleanroom procedures and to use equipment in the laboratory for their research.

The remaining budget will be used to purchase necessary “100 class” furniture, supplies and standard cleanroom instruments.

The views of the Nanodevice Processing Laboratory are presented in Figs 1 and 2.

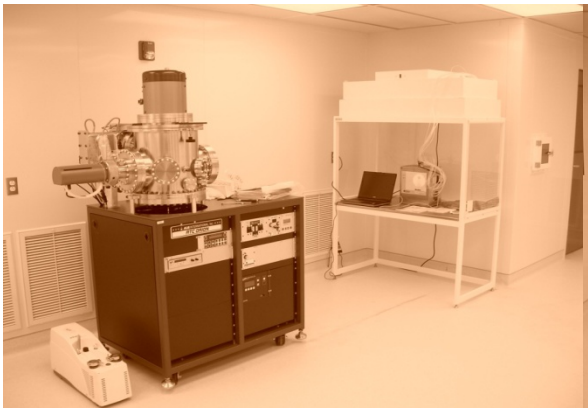

Fig1. Ion milling system and a particle monitoring system (inside the vertical flow-bench in the Nanodevice Processing Laboratory

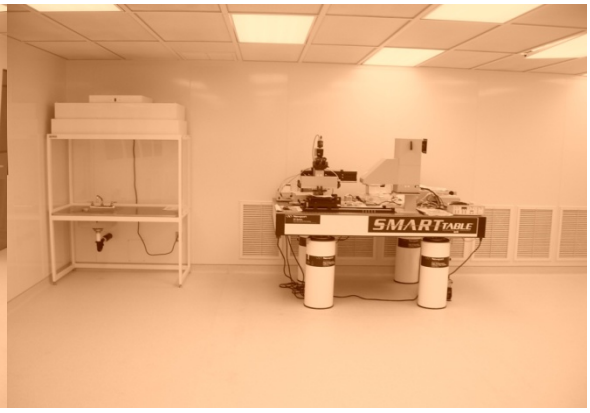

Fig 2. Mask aligner/ UV exposure station mounted on anti-vibration table.

Project Revision

The design of the clean laboratory using recirculating air made it possible to exceed the originally planned standards of the cleanroom class1000. As a result, the Nanodevice Processing Laboratory meets standards of higher class 100 cleanroom (or ISO class 5).